筑　波　大　学

博 士 （医 学） 学 位 論 文

Analysis of the mechanism of functional endothelial progenitor cells *in vivo*

生体内における有用性血管内皮前駆細胞の機能解析

２０１６

筑波大学大学院博士課程人間総合科学研究科

TRAN CAM TU

Thesis Abstract

Background

Over the last decade, adult stem cells have been proposed as novel targets of cell therapy. Endothelial progenitor cells (EPCs) with low aldehyde dehydrogenase activity (Alde-Low EPCs) are known to be suitable for the treatment of ischemic tissue whereas EPCs with high aldehyde dehydrogenase activity (Alde-High EPCs) are non-functional which cannot promote wound healing in mouse flap model. However, how Alde-Low EPCs contribute to wound healing is not fully understood. Moreover, stem cell-derived microvesicles (MVs) are capable of carrying functional mRNAs, miRNAs and proteins to target cells through the way of horizontal transfer and play critical role in cell-cell communication. Thus, extracellular vesicles are emerging as potent genetic information transfer agents underpinning a range of biological processes and with therapeutic potential.

Purposes

In this thesis work, the first aim is to investigate how Alde-Low EPCs as well as their MVs contribute to ischemic tissue repair. The second aim is to clarify the key molecules that are involved in the recovery from tissue damage. The third aim is to find a genetic tool to improve wound healing ability of Alde-High EPCs and Adipose tissue derived mesenchymal stem cells (AT-MSCs).

Materials and methods

I carried out cell culture protocol and FACS analysis to prepare target cell population such as EPCs, AT-MSCs. To isolate MVs, I performed ultracentrifugation. I used real

time- polymerase chain reaction to examine the mRNA and miRNA expression, western blotting to evaluate protein expression levels and chromatin immunoprecipitation (CHIP) assay to detect interaction between DNA and protein. HIF-1α, HIF-2α as well as CXCR4, VEGF was knockdown in Alde-Low EPCs by short hairpin RNA (shRNA). *In vitro* and *in vivo* migration assay were used to check the migratory ability and ischemic tissue recover of target cells. Finally, data were statistically analyzed using Student's *t*-test or a one-way analysis of variance as appropriate. Data are presented as the mean ± SD.

Results

The expression level of HIF-1α and HIF-2α were found to be significant higher in Alde-Low EPCs than in Alde-High EPCs. Interestingly, Alde-High EPCs with MVs derived from Alde-Low EPCs improved their ability to repair an ischemic skin flap, and the expression of CXCR4 and its ligand SDF-1 was significantly increased following the coculture. In Alde-Low EPCs, the expression of CXCR4 was suppressed by shRNA-HIF-2α, but not shRNA-HIF-1α. CHIP assay showed that HIF-2α binds to the promoter region of CXCR4 gene. The CXCR4 shRNA treatment in Alde-Low EPCs almost completely abrogated their migratory activity to ischemic tissues. The CXCR4 overexpression in Alde-High EPCs resulted in a partial, but significant improvement in their repairing ability in an ischemic skin flap. In addition, I also demonstrated that MVs derived from Alde-Low EPC possessed the ability to improve the homing capacity of AT-MSCs, resulting wound healing. Remarkably, the expression of CXCR4 is highly elevated in MV-transfected AT-MSCs. Moreover, AT-MSCs transfected with MVs

showed migration at the sites of wound after their intravenous injection. Consequently, $CD45^+$ inflammatory cells were successfully recruited at wound sites after the injection of MVs-transfected AT-MSCs.

Discussion

Here, I indicated that while both HIF-1α and HIF-2α have an important role in the recovery from ischemia, the role of HIF-2α in association with EPCs would be crucial during the process of ischemic tissue repair. The ischemic tissue fully recovered after the transplantation the MV-transfected Alde-High EPCs. In addition, I showed that MVs from Alde-Low EPCs provide an important potential as a therapeutic tool for AT-MSCs. AT-MSCs that was originally unable to repair the wound when transplanted intravenously became to migrate at the wound sites after the incorporation of MVs derived from Alde-Low EPCs. The significant upregulation of CXCR4 was observed in AT-MSCs transfected MVs. It has been reported that SDF-1 is secreted at the site of skin flap dependent on degree of low oxygen tension. Thus, AT-MSCs highly expressing CXCR4 may be attracted and migrated to the wound sites where the expression of SDF-1 is upregulated.

Conclusion

I proved the crucial role of CXCR4 expressed in Alde-Low EPCs in the process of ischemic tissue repair. The CXCR4/SDF-1 axis, which is specifically regulated by HIF-2α, plays a crucial role in the regulation of EPC migration to ischemic tissues. Additionally, MVs derived from Alde-Low EPCs are a useful source to gain the properties, which possess the homing capability and effective wound healing ability at the injured sites**.**

TABLE OF CONTENT

CHAPTER 1. INTRODUCTION

1. Background

1.1 Endothelial progenitor cells

Endothelial progenitor cells (EPCs) were first isolated from adult peripheral blood (PB) in 1997 [1] and were shown to derive from bone marrow (BM). It has reported that EPCs have ability to incorporate into focus of physiological or pathological neovascularization [2, 3]. Moreover, a postnatal neovascularization was originally found to be constituted by the mechanism of angiogenesis, this process was controlled by in situ proliferation and migration of pre-existing endothelial cells [4]. Therefore, the discovery of EPCs has drastically changed the understanding of adult blood vessel formation.

1.1.1. Defining endothelial progenitor cells

Until now, the definition of an EPC has been controversial and since the method to isolate EPCs has been variable among investigators [5]. Several researches have been reported that there are two distinct types of EPCs which are called early and late EPCs according to the appearance sequentially [6]. Early EPCs, are characterized by the expression of CD45 and CD14, likely originating from monocytic/dendritic cells, together with some endothelial cell (EC) markers, and have a short lifespan of three to four weeks. Whereas, late EPCs rapidly grow out from mononuclear cells with a cobblestone-like morphology and are characterized by

EC markers such as CD31, CD34, VEGFR2, and VE-cadherin, but are negative for myeloid markers [6]. However, Yoder *et al.* have recently demonstrated that stock of the $CD45^{+}CD14^{+}$ cells that co-express EC markers are not endothelial progenitor cells but hematopoietic-derived myeloid progenitor cells [7]. Alternatively, it has been reported that ECs were divided into several subpopulations according to their clonogenic and proliferative potential [8]. They identified a population of highly proliferative endothelial potential–colony-forming cells, which form secondary colonies in human UCB. For the therapeutic potential of EPCs, the effective isolation of highly proliferative EPCs is centrally important for the generation of reliable and safe cell-based therapy.

1.1.2 Separation of endothelial progenitor cells based on ALDH activities.

Aldehyde dehydrogenase (ALDH) has an ancient origin and is found in all living organisms from Archaea and Eubacteria to eukaryotes [9, 10]. The human genome and expression researches revealed that there are 19 functional ALDH genes with a wide range of tissue expression and substrate specificity. ALDH is an enzyme responsible for oxidizing intercellular aldehydes [11]. This enzyme plays an important role in ethanol, vitamin A and cyclophosphamide metabolism [12, 13, 14]. Although ALDH is a cytosolic protein, its expression level can be monitored by flow cytometry using the fluorescent aldehyde called dansyl aminoacetaldehyde (DAAA, also known as Aldefluor) [15]. Several studies have been shown that hematopoietic stem cells, hematopoietic progenitor cells and intestinal crypt stem cells express high

level of ALDH [16]. Lyle Amstrong *et al.* reported that hematopoietic stem cells with high level of ALDH activity were isolated from UCB [17].

Nagano *et al.* previously demonstrated that aldehyde dehydrogenase 1 (ALDH1) activity was a useful marker for separating functional EPCs from the whole endothelial colony-forming cell population [18]. Alde-Low EPCs have been shown to promote significantly better wound healing in a mouse model of skin flap ischemia. This improved wound healing was not observed with human umbilical vein endothelial cells (HUVECs) or Alde-High EPCs. Alde-Low EPCs were also found to grow faster, have a greater capacity to migrate to ischemic sites, and to be directly involved in new vessel formation [18].

In addition, the separation of EPCs based on ALDH activity shows following advantages: 1) ALDH activity was retained in low or high in EPCs after several passages, 2) staining protocol was easily adopted without excessive cellular manipulation, 3) Adlefluor was not intercalated into DNA [18].

1.1.3. Functional properties of endothelial progenitor cells

1.1.3.1 Endothelial progenitor cell mobilization

Actually, the bone marrow is home to a stem cell niche which consists of fibroblast, osteoblast, endothelial cells and will provide an environment of self-renewal and differentiation of progenitor and stem cell. Mobilization of endogenous EPCs from the bone marrow may be an alternative way to increase postnatal

neovascularization. Progenitor cells are mobilized from bone marrow into the circulation in response to a number of cytokines and growth factors included Vascular Endothelial Growth Factor (VEGF), Stromal cell Derived Factor (SDF), angiopoetin 1 and erthyropoetin [19]. Both VEGF and SDF-1 upregulate bone marrow MMP9- activity, resulting in progenitor mobilization into the vascular area of bone marrow [19]. In addition, tissue hypoxia appears to be a major stimulus for VEGF release, mostly due to the increasing of VEGF mRNA levels in response to hypoxia inducible factor 1 (HIF-1α) [20]. Animal studies demonstrated that the mobilization of EPCs is increased in response to VEGF [21]. Recently, some evidences have shown that erythropoietin is another cytokine that mobilization EPCs *in vivo* [22, 23].

Recently, EPCs circulate in the blood and possess the ability to differentiate into mature vascular endothelial cells (ECs), contribute to new vessels, and to aid in the regeneration of impaired blood vessels [24, 25].

1.1.3.2. Endothelial progenitor cells adhesion

In order to participate in vascular repair, EPCs need to adhere to the vasculature at the site of ischemia or injury. Intergrins have been demonstrated to mediate adhesion of endothelial cells. In details, ß-1-intergrins are expressed on the surface of endothelial cells while ß-2-intergrins are expressed on hematopoietic stem cells [26]. ß-2-intergrins are also expressed on the surface of EPCs derived from peripheral blood and required for EPC adhesion to endothelial cells and trans-

endothelial migration *in vitro* [27].

1.1.3.3. Endothelial progenitor cell chemotaxis and migration

In order to response the tissue injury and ischemia, a number of EPCs are released, it is necessary to have a sufficient concentration of chemo-attractant factors to facilitate recruitment to the injured site. VEGF has been demonstrated to act as a chemo-attractant factor to EPCs [28]. In addition, SDF-1 has been shown to be an important chemotactic factor and stimulates recruitment of EPCs to ischemic tissue [29, 30]. Recent studies have shown that SDF-1 plays an important role in the regulation of a variety of cellular functions of EPCs such as cell migration, proliferation, and survival. Interestingly, CXCR4, a transmembrane-spanning G protein-coupled receptor, is the receptor for SDF-1 and is the most important homing gene of EPCs [30].

1.1.3.4. Endothelial progenitor cells and angiogenesis

It has been suggested that bone marrow-derived EPCs localize within the site of EC damage and induce revascularization [31]. Indeed, after EPCs pass from bone marrow to peripheral circulation, they migrate to the sites at which endothelial injury and a hypoxic state occur within the tissue. Once there, EPCs promote angiogenesis with or without directly contributing to the formation of vessels in response to the physiologically distinct environment [27, 32, 33] (Figure 1).

The mechanisms by which EPCs are able to induce recovery in damaged vessels and tissues are not fully understood. Several studies have demonstrated that

EPC infusion exerts protective effects on hindlimb ischemia, myocardial infarction, and glomerular diseases in animal models [33]. Despite these benefits, the regenerative effects of EPC-based cell therapy remain to be clarified: whether EPCs directly contribute to and are incorporated in revascularization [34, 35] or whether they favor reciprocal interaction due to a paracrine mechanism that occurs within ischemic tissues [36]. Recently, many studies have suggested that cells may also communicate through circular membrane fragments named microvesicles (MVs) [37]. It has been hypothesized that MVs released from EPCs may play an important role in the cell-to-cell communication of cytokines, growth factors, surface receptors, and nucleotides [38, 39].

In addition, hypoxia is an important point of homeostatic mechanisms of the regulation of angiogenesis [40]. It is reported that Hypoxia-inducible factor (HIF) is an α,β-heterodimeric transcription factor that mediates cellular responses to low oxygen concentration via the transcriptional activation of specific genes involved angiogenesis. Study of the HIFs pathway has potential use for the treatment of ischemic disease and cancer [41].

1.1.4. Perspective for future direction.

Although there are many encouraging studies regarding the therapeutic potential of EPCs, several issues currently needed to be studied in the way of their wide clinical application. Strategies need to be developed to enhance the number of EPCs as well as source of cells such as bone marrow, umbilical cord blood, umbilical

cord vein and peripheral blood. Moreover, further examination of the biology of EPCs need to be determined about the nature of the mobilizing, migratory and homing signal, and the mechanism of incorporation into the target tissues. I listed some issueses which need to standardize in order to apply EPCs for treatment of tissue ischemia, and vessel repair or angiogenesis. Despite these hurdles, the application for EPC-based therapy for tissue ischemia and blood vessel repair appears promising. Genetic engineering of EPCs may provide an important strategy to enhance EPC mobilization, survival, engraftment, and function, thereby rendering these cells efficient therapeutic modalities for ischemia or cardiovascular disease.

1.2. Mesenchymal stem cells

The non-hematopoietic stem cells in bone marrow was first discovered by the study of the German pathologist Cohnheim. His research showed the capacity of bone marrow that can be used as the source of fibroblast that deposit collagen in the process of wound repair [42]. After separation by density gradient centrifugation, human mesenchymal stem cells (MSCs) are typically isolated from the mononuclear layer of the bone marrow [43]. The mononuclear cells are cultured in medium with 10% fetal bovine serum, and the MSCs adhere to the tissue culture plastic. Some hematopoietic cells also adhere, but after few passages in culture these are washed away. MSCs have now been isolated from various sites other than the bone marrow, including adipose tissue, amniotic fluid, periosteum, and placenta [44, 45, 46, 47].

Among the adult stem cells, MSCs have been considered as an excellent material for regenerative medicine because of their self-renew ability, broad differentiation potential, wide accessibility and lack of ethical concerns [48, 49]. In addition to multi-potent potential, MSCs can regulate immune/ inflammatory processes making these cells more attractive for the therapy of many disorders [50, 51, 52].

Adipose tissue-derived MSCs (AT-MSCs) are expected as more reliable cell source for regenerative medicine because that can be isolated by minimally invasive fashion for the patient compared to other MSCs [49]. There are multi-steps for MSCs to engraft to the appropriate sites after the delivery from some particular organs where MSCs are located. It is especially important to investigate the MSC properties in each situation in our body in the multi-steps, such as extravasations, homing and engraftment of MSCs. However, few studies have provided insight into the mechanisms of MSCs to improve the therapeutic efficacy.

1.3. Microvesicles (MVs)

Extracellular vehicles have been considered as bioactive mediators of cell-cell interaction. These vehicles are categorized into exosomes and shedding vehicles. The mixed populations of exosomes and shedding vehicles are collectively known as microvesicles (MVs). MVs are a heterogeneous population of membrane vesicles that are shed or bud from the cell membrane (Figure 2). Since they shed directly from the plasma membrane, one could expect the composition of shedding vesicles to be comparable to the membrane composition of the cells of origin [53]. Recently, MVs

can be isolated using ultracentrifugation (Figure 3). MVs contain surface receptors, bioactive molecules such as proteins and lipids as well as mRNAs and microRNAs [37, 38]. Therefore, those RNAs in MVs could play a role in the exchange of genetic material between stem cells and target cells as well as the changing of biological activity by proteins or lipids. Since, MVs seem to be nature's way to deliver biological items, they hold great potential as a novel class of drug delivery systems [53].

It has been shown that MVs derived from EPCs activated an angiogenic program in endothelial cells by a horizontal transfer of mRNA [38]. To develop a unique gene therapy, it would be necessary to investigate therapeutic power of MVs derived from many types of stem cells in future.

2. Abbreviations

ALDH	Aldehyde dehydrogenase
ATMSCs	Adipose tissue derived mesenchymal stem cells
b-FGF	basic Fibroblast growth factor
BM	Bone marrow
BSA	Bovine serum albumin
CCL	chemokine (C-C motif) ligand
cDNA	Complementary DNA

CHIP	Chromatin immunoprecipitation
ColIV	Collagen type IV
CXCR4	C-X-C chemokine receptor type 4
DFO	Desferrioxamine
ECs	Endothelial Cells
EPCs	Endothelial Progenitor Cells
FACS	Fluorescence-activated cell sorting
FBS	Fetal bovine serum
GFP	Green fluorescent protein
Glut-1	Glucose transporter 1
HIF	Hypoxia inducible factor
HUVEC	Human umbilical vein endothelial cells
IMDM	Iscove's modified Dulbecco's medium
IL6	Interleukin 6
MSCs	Mesenchymal stem cells
miR	Micro-RNA
mRNA	messenger RNA
MVs	Microvesicles

PBS	Phosphate-buffered saline
PB	Peripheral blood
RT-PCR	Reverse transcription-polymerase chain reaction
shRNA	Short hairpin RNA
SDS-PAGE	Sodium dodecyl sulfate–polyacrylamide gel electrophoresis
SDF-1	Stromal cell derived factor 1
TGF	Transforming growth factor
UCB	Umbilical cord blood
VCAM-1	Vascular cell adhesion molecule 1
VEGF	Vascular endothelial growth factor

3. Aim of study

Our group has clearly demonstrated that Alde-Low EPCs are suitable for the treatment of ischemic tissue whereas Alde-High EPCs cannot promote wound healing in mouse flap model [18]. However, how Alde-low EPCs contribute to wound healing is not fully understood. I took note of the fact that MVs are capable of transferring bioactive molecules including mRNAs, miRNAs and proteins to recipient cells and play critical role in cell-cell communication. Therefore, Alde-Low EPC-derived MVs could be expected as potent genetic information transfer agents underpinning a range of biological processes and with therapeutic potential. In my PhD work, I have following purposes as listed bellow:

1. Investigate a functional role of Alde-Low EPCs to contribute into ischemic tissues
2. Find key molecules involved in the wound healing process in Alde-Low EPCs
3. Examine a function role of Alde-Low EPCs-derived microvesicles to promote the migration and wound healing ability of Alde-High EPCs and AT-MSCs.

Chapter II. Materials and Methods

1. The preparation of EPCs isolated by ALDH activity

Human full-term UCB samples (n = 3) were collected from umbilical cord veins with the permission of the local ethics authorities at the University of Tsukuba. Mononuclear cells from human UCB were separated by density gradient centrifugation after the depletion of hematopoietic cells. $CD45^{-}/CD31^{+}$ cells were then sorted using anti-CD45 and anti-CD31 antibodies (BioLegend) with a MoFlo (MoFlo XDP; Beckman Coulter). Cells were plated on a 25-cm^2flask (Sumitomo Bakelite) with Iscove's modified Dulbecco's medium (IMDM; Life Technologies) with 10% fetal bovine serum (FBS; Life Technologies), 2 mg/mL L-glutamine (Life Technologies), 10 ng/mL hb-FGF (PeproTech), and 0.1% (vol/vol) penicillin–streptomycin (100 U/mL penicillin, 0.1 mg/mL streptomycin; Life Technologies) as described previously [18]. After 7 days, adherent cells began to grow and rapidly evolve to form colonies with tightly compact morphologies. Subsequently, DiI-Ac-$LDL^{+}/CD31^{+}$ cells were sorted (DiI-Ac-LDL; Molecular Probes) with a MoFlo. The culture of the sorted cells was continued in IMDM/10% FBS supplemented with b-FGF [18]. These cells displayed an EC-like morphology. Their ALDH activity was analyzed with an ALDEFLUOR® (StemCell Technologies). The EPCs were then sorted into two fractions based on their level of ALDH expression (Alde-High EPCs and Alde-Low EPCs) using the MoFLo. The EPCs were labeled with the lentivirus-

green fluorescent protein (GFP) (Sigma-Aldrich) in order to use in the experiment of *in vivo* migration assay. Frozen cell stocks were prepared using the CELLBANKER (ZENOAQ) solution and stored in liquid nitrogen. For hypoxic stimuli, EPCs were treated with or without desferrioxamine (DFO: 100 μM) for 6 h or cultured under hypoxic conditions (1% O_2) for 6 h.

2. Microvesicle (MV) preparation and transfection protocol

MV isolation was performed according to the method reported by Deregibus *et al.* [34] with some modifications. After EPCs reached confluence, the culture medium of EPCs was changed to serum-free EBM-2 (Lonza, Basel, Switzerland) supplemented with 0.25% BSA (Sigma-Aldrich, St. Louis, MO). After 12 h, supernatants were collected and centrifuged at 1,000 x g for 20 minutes to remove debris and ultracentrifuged at 100,000 x g (Beckman Coulter Optima L-100K) for 60 min at 4^{o}C. MV pellets were washed with PBS and re-centrifuged at 100,000 x g for 60 min at 4^{o}C. MVs were purified using a cell sorter (MoFlo XDP) according to the expression of EPC-specific markers. The antibodies used were PE–labeled anti-CD31, APC–labeled anti-CD45 (BioLegend, San Diego, CA) and FITC-labeled anti-CD105 (Serotec, Oxford, UK). The protein content of MVs was quantified using the Bradford method (BioRad). MVs were stained using the PKH26 red fluorescent cell linker kit for general cell membrane labeling (PKH26GL-1KT -100M0612- Sigma-Aldrich) or PKH67 green fluorescent cell linker kit for general cell membrane labeling (MINI 67-1KT - SLBB7129- Sigma-Aldrich). After the staining, MVs were

washed twice by PBS using ultracentrifugation before incubation with recipient cells. The labeled MVs were mixed in culture medium and incubated with Alde-High EPCs or AT-MSCs (14.5 μg/ 500,000 cells). The efficiency of transfected cells was examined using FACSs according to the fluorescent signal after 12 h of MV transfection.

3. Quantitative RT-PCR

RNA was isolated from cultured cells or MV samples using an RNeasy Mini Kit (Qiagen). Total RNA (1 μg) was reverse transcribed using an RT-PCR Kit (TOYOBO). Complementary DNA (cDNA) was analyzed using a GeneAmp 7500 Fast Real-Time PCR System (Life Technologies) using the SYBR Green reagent (TOYOBO). The expression levels of the target genes were analyzed with the ΔΔCt method. The primers used for the polymerase chain reaction (PCR) were as follows: VEGF (5′-AGATGAGCTTCCTACAGCACAAC; 3′-AGGACTTATACCGGGATTTCTTG), CXCR4 (5′-CTGTGACCGCTTCTACCCCAATGACTT; 3′-CCAAGGAAAGCATAGAGGATGGGGTTC), KDR (5′-AGTGTGGAGGACTTCCAGGGAGGAAAT; 3′-GGCCAAGCTTGTACCATGTGAGGTTCT), SDF-1 (5′-TGAGAGCTCGCTTTGAGTGA; 3′-CACCAGGACCTTCTGTGGAT), VCAM-1 (5′-GTAAGCTGCAAGGTTCCTAGCGTGT; 3′-GCTGACCAAGACGGTTGTATCTCTG), Glut-1 (5′-

ACTGCTCAAGAAGACATGGAGAC; 3′-ATTTACAAGTTGGCTTGTCCAGA), TGF-β (5′-AGAGCTCCGAGAAGCGGTACCTGAACCC; 3′-GTTGATGTCCACTTGCAGTGTGTTATCC), HIF-1α (5′-TTACCGAATTGATGGGATATGAG; 3′-TCATGATGAGTTTTGGTCAGATG), ColIV (5′-AGGGCCAGCCTGGCCTGCCAGGACTTCC; 3′-TCACCCTTAGAGCCTGTGATTCCTGGAG), CoIV (5'-AGGGCCAGCCTGGCCTGCCAGGACTTCC; 3'-TCACCCTTAGAGCCTGTGATTCCTGGAG), hCCL2 (5'-ATGAAAGTCTCTGCCGCCCTTCTGTG; 3'-TCAAGTCTTCGGAGTTTGGGTTTGCTT), hCCL5 (5'-GAGGATTCCTGCAGAGGATCAAGACAG, 3-TCCAAAGAGTTGATGTACTCCCGAACC),

hCCL3 (5′-ACTGCCTGCTGCTTCTCCTACA- 3′-AGGAAAATGACACCTGGCTGG),

and β-actin (5′-GTGCGTGACATTAAGGAGAAGCTGTGC; 3′-GTACTTGCGCTCAGGAGGAGCAATGAT).

4. RT-PCR for miRNAs

The miRNA quantification using the Tagman miRNA assays was determined by two-step RT-PCR following the manufacture's protocol. The real time was performed using the Tagman miRNA reverse transcription kit and the PCR step was performed using Tagman universal PRC master mix II, with UNG. The primers for

miRNAs include hsa-miR-126 (P140423-005 G01), has-miR296 (P140625-000-E03) and RNU48 (P141013-007 E07) (Applied Biosystems).

5. Animal studies

C57BL/6J male mice (8 to 10 weeks) were purchased from Japan SLC, Inc. The mice were treated in accordance with the National Institutes of Health (NIH) Guide for the Care and Use of Laboratory Animals. All animal studies were performed after receiving approval from the Institutional Animal Experimental Ethics Committee of the University of Tsukuba.

The mice were anesthetized with Avertin and the back skin was shaved. To create the ischemic region, a rectangular-shaped incision (3 × 2 cm) was made on the dorsal skin with only the proximal end remaining attached to the circulation, thus creating a proximal to distal ischemic gradient [34]. Immunosuppression was induced by an intraperitoneal injection of cyclosporin-A (20 mg/kg/day) (Wako) from 2 days before the assay [8]. Following surgery, GFP-labeled EPCs or AT-MSCs with or without MVs transfection (5×10^5 cells/mouse) were injected into the tail vein. After 7 days of the surgery/injection, mice were sacrificed and the image of necrotic skins was captured. The necrotic areas and total area of skin flap were measured. Then the necrotic areas were divided to total area of skin flaps. The results are expressed as the average area of necrotic skin as a percentage of the total flap area. An *in vivo* migration assay was carried out at 24 h after the GFP labeled EPCs or AT-MSCs plus MVs injection. To detect GFP-labeled EPCs, AT-MSCs plus MVs, frozen flap skin

tissue sections were analyzed by a fluorescent microscopy to detect fluorescent signals. The results are expressed as the average number of cells that were seen as per high-power field.

6. Western blotting

Sample cells, which were treated with or without DFO (100 μM) for 6 h, were harvested and suspended in low salt buffer [10 mM HEPES, 10 mM KCl, 1 mM dithiothreitol, 0.1 mM EDTA, protease inhibitor cocktail (PIC; Roche Diagnostics), and 1% Nonidet P-40] and nuclear pellets were collected by centrifugation. The nuclear pellets were suspended in high salt buffer (20 mM HEPES, 400 mM NaCl, 1 mM dithiothreitol, and 1 mM EDTA, PIC); after centrifugation, a nuclear extract was obtained. These nuclear extract samples were separated on 10% sodium dodecyl sulfate–polyacrylamide gel electrophoresis (SDS-PAGE) gel by electrophoresis and transferred onto PVDF membrane (Millipore). An immunoblotting analysis was performed as previously described [18]. Anti-human HIF-2α antibody [56], anti-human HIF-1α antibody (Novus Biologicals), and anti-Lamin B antibody (Santa Cruz Biotechnology, Inc.) were used for the immunoblotting assay. Horseradish peroxidase (HRP)-conjugated goat anti-rabbit IgG (Invitrogen) or goat anti-mouse IgG (Life Technologies) was used as the secondary antibody, and enhanced chemiluminescence (GE Healthcare Biosciences) was used for detection.

7. Overexpression and the shRNA treatment of target genes

The Alde-High EPCs were infected using cell-free retroviral supernatant from

PT67 packaging cells (Clontech) producing MSCV-hCXCR4-IRES-EGFP or MSCV-IRES-EGFP (control virus) with 8 mg/mL polybrene. After 24 h, the medium was changed to fresh virus-free medium, and cells were expanded for 4–6 days. The GFP-positive cells were then sorted using a MoFlo and then expanded for the subsequent experiments. MSCV-hVEGF-PGK-puro retroviruses were used to promote VEGF overexpression in Alde-High EPCs. Puromycin (2 μg/mL) was used to select infected EPCs.

To downregulate the target genes, I used the shRNA MISSION lentiviral transduction system (Sigma-Aldrich) according to the manufacturer's protocol. The infected cells were selected with a puromycin resistance method. Puromycin (2 μg/mL) was used to select the infected EPCs.

8. Chromatin immune-precipitation assay

For each assay, 5×10^6 Alde-Low EPCs were fixed with 1% formaldehyde for 10 min at room temperature. After being washed with PBS containing 1 μM PIC (Roche Diagnostics), the EPCs were treated with hypotonic solution (5 mM HEPES, 85 mM KCl, 0.5% NP-40, and 1 μM PIC). Nuclei were collected after centrifugation at 14,000*g* for 5 min, then lysed with a lysis buffer (50 mM Tris-HCl, [pH 8.1], 10 mM EDTA, 1% SDS, and 1 μM PIC). After the fragmentation of DNA by sonication, immunoprecipitation reactions were performed using a rotating mixer at 4°C with 1 μg/mL anti-HIF-1α antibody or anti-HIF-2α antibody (Novus Biologicals). Normal mouse IgG or rabbit IgG was used as a negative control to

verify the specificity of the reaction. After incubation with the antibody, reaction mixtures were incubated with preblocked protein A agarose beads (Calbiochem) at 4°C for 1 h and the precipitated complexes were collected by centrifugation at 3,000*g* for 5 min. These complexes were washed three times with the wash buffer (0.25 mM LiCl, 1% NP-40, 1% sodium deoxycholate, 1 mM EDTA, and 10 mM Tris-HCl [pH 8.1]) and eluted from the protein A agarose beads with the elution buffer (1% SDS and 0.1 M NaHCO3). DNA–protein complexes were denatured by incubation at 65°C for 4 h. DNA fragments were purified with phenol/chloroform, and resuspended in the TE buffer. The following primers were used for the PCR: forward, 5′-TTCTTCAACCTAATTTCTGATTCGTGC-3′ and reverse, 5′-ATCACTAGGAACTTGCACAGAATCAC-3′.

9. *In vitro* migration transwell assay

This assay was perform follow the protocol which was originally introduced by Boyden with some modification [57]. EPCs (5×10^4 cells) were seeded onto transwell (6.5 mm, 8 μm pore; BD Biosciences) in IMDM supplemented with 0.5% FBS. IMDM/0.5% FBS with recombinant human SDF-1 (200 ng/mL; R&D Systems) was added to the lower chamber. The assays were performed under different oxygen tensions (20% or 5%) for 6 h, and non-migrated cells were wiped away from the top surface of the membrane. Cells that adhered to the undersurface of the membrane were stained with Diff-Quik staining solution (International Reagents) and then counted using an inverted microscope.

10. Preparation of MSCs derived from adipose tissue

Human adipose tissue samples (n = 3) of healthy donor were collected after informed consent with permission from the local ethics authorities at the University of Tsukuba. The protocol for isolation of AT-MSCs was follow from protocol [37]. Tissues were minced and treated with 10% collagenase 0.1% (Nitta Gelatin, Osaka, Japan) in 20% fetal bovine serum (FBS; Hyclone SH30396.03, South Logan, UT) and 70% phosphate buffer saline containing 0.1% (vol/vol) penicillin-streptomycin (Invitrogen 15140; 100 U/mL penicillin, 0.1 mg/mL streptomycin, Carlsbad, CA) at 37^{o}C for 40 min. A single cell suspension was made using a syringe and 18G needle, then filtered through a cell strainer (Falcon; pore size 100 μm, BD Bioscience, San Joe, CA), followed by centrifugation at 1500 rpm at 10^{o}C for 5 min. Cells were cultured in *Iscove's Modified Dulbecco's Medium* (IMDM; Invitrogen 12200-069), 10% FBS, 2 mg/mL L-glutamine (Invitrogen; 25030), 5 ng/mL recombinant human b-FGF (Peprotech; 064-04541, London, UK) at 37°C in 5% CO_2 and a humidified atmosphere. After 1 day, medium containing non-adherent cells was removed and replaced with fresh medium. Frozen cell stocks were prepared using Cell Banker solution (ZENOAQ, Koriyama, Japan) and stored in a −80^{o} C freezer and liquid nitrogen for further experiments.

11. *In vitro* differentiation assay of MSCs

To induce osteogenic differentiation, 5x10^{4} cells were treated with osteogenic differentiation medium in 4-well plates (Nalge Nunc, Rochester, NY) for 4 weeks.

The osteogenic differentiation medium consisted of IMDM supplemented with 1% FBS, 0.1 mM dexamethasone (Sigma–Aldrich), 10 mM β-glycerol-2-phosphate (Sigma–Aldrich), 0.2mM ascorbic acid (Sigma Aldrich) and 50 ng/ml of human EGF [13, 20]. The culture medium was replaced with fresh medium once or twice a week. The mineralized matrix was evaluated by Von Kossa staining and Alizarin red staining as described previously [57, 58].

Adipogenic differentiation was induced in 4-well plates for 4 weeks by adipogenic differentiation medium consisting of IMDM supplemented with 10% FBS, 0.1 mM dexamethasone (Sigma–Aldrich), 0.5 mM 3-isobutyl-1-methylxanthine (IBMX; Sigma–Aldrich), 2 mg/ml insulin (Wako) and 0.1 mM indomethacine (Sigma–Aldrich). The culture medium was replaced with fresh medium once or twice a week. Cultured cells in adipogenic differentiation medium were fixed with 10% formaldehyde and stained with Oil-Red O solution (Muto Pure Chemicals, Tokyo, Japan) for 30 min at 42^{o}C. After the staining, cells were dissolved with 4% IGEPAL CA630 (Sigma–Aldrich) in isopropanol and the absorbance was measured at 480 nm.

12. *In vitro* migration scratch assay with mytomicin C

The *in vitro* migration assay was performed according to the modified method reported by Chun-Chi Liang *et all.* [59]. Briefly, AT-MSCs ($1.5x10^5$ cells) were seeded on 4-well dish (BD Biosciences) in IMDM supplemented with 10% FBS. After cells reach confluent monolayer, cells were inactivated by mytomicin C (Sigma) at concentration 10 μg/ml for 3 h. Cells were washed three times with PSB

and scratch wounds of 1 mm width were generated with a 200 μm pipette tip. Cells were wash 2 times with PBS softly to remove all floating cells. AT-MSCs were then transfected with or without MVs derived from Alde-low EPCs, and cultured for 16 h. Representative pictures were captured to track migration of individual cells in the leading edge of the scratch. Migration distance (μm) was calculated by software ImageJ.

13. Histological analysis

Inflammatory cells in the ischemic tissue were examined by immunohistochemical staining with PE-labeled anti-CD45 (30F11, BD Pharmingen). The number of CD45-positive cells was counted in each field. The presented data are the average of ten fields per section.

14. Statistical analysis

Data were statistically analyzed using Student's *t*-test or a one-way analysis of variance as appropriate. Data are presented as the mean ± standard deviation.

Chapter III. A Chemokine Receptor, CXCR4, Which Is Regulated by Hypoxia-Inducible Factor 2α, Is Crucial for Functional Endothelial Progenitor Cells Migration to Ischemic Tissue and Wound Repair

1. Purpose

EPCs have the ability to form new blood vessels and protect ischemic tissues from damage. We previously reported that EPCs with low activity of aldehyde dehydrogenase (Alde-Low EPCs) possess the greater ability to treat ischemic tissues compared with Alde-High EPCs. However, the mechanisms by which EPCs are able to induce recovery in damaged vessels and tissues are not fully understood.

Recently, many studies have suggested that cells may also communicate through circular membrane fragments named microvesicles (MVs). It has been hypothesized that MVs released from EPCs may play an important role in the cell-to-cell communication of cytokines, growth factors, surface receptors, and nucleotides.

The aim of this study was to investigate how functional EPCs (Alde-Low EPCs) as well as their MVs contribute to ischemic tissue repair and to clarify the key molecules that are involved in the recovery from tissue damage.

2. Results

2.1. Alde-High EPCs with MVs derived from Alde-Low EPCs possess the ability to repair wounds

Alde-High EPCs and Alde-Low EPCs were derived from the same UCB samples and separated with fluorescence-activated cell sorting on the basis of ALDH activity, as previously reported. The ratio of Alde-High EPCs was 24.6% ± 9.4%, whereas the ratio of Alde-Low EPCs was 37.3% ± 1.5% [18]. To characterize the cell types, we investigated whether Alde-High EPCs could attain similar characteristics to Alde-Low EPCs through exterior influences.

MVs are released from the cell surface and are able to transfer mRNAs and miRNAs between cells. The release of MVs from the cell surface increases cell growth activity, reduces apoptosis, and protects from cellular injury [60, 61].

I first isolated MVs derived from Alde-Low EPCs (Fig. 3) by ultracentrifugation 2 times, then MVs were mixed in culture medium and incubated with Alde-High EPCs. In contrast to Alde-Low EPCs, Alde-High EPCs have not been shown to promote wound healing.

The isolation of MVs from Alde-Low EPCs was performed with reference to previous reports and evaluated by examining the expression of angiogenic genes in the MVs. As shown in Fig. 4C, PKH26-labeled MVs, which were isolated from Alde-Low EPCs, were incorporated in Alde-High EPCs by coculture for 12 h. The expression of MVs in relation to the angiogenic genes was analyzed; most of the

examined genes were positively expressed similar to those in their parent cells (Alde-Low EPCs) (Fig. 4B).

I then examined the expression of angiogenic genes in Alde-High EPCs that were cocultured with MVs derived from Alde-Low EPCs. The expression of the CXCR4 chemokine receptor, which is important for migration at the wound site, and its ligand SDF-1, were found to be highly elevated in the MVs transfected Alde-High EPCs.

Angiogenic factor, VEGF, and adhesion molecules, Col IV and VCAM-1, were also upregulated in the transfected Alde-High EPCs in comparison to the nontransfected Alde-High EPCs (Fig. 5). An *in vivo* assay using a mouse model of skin flap ischemia clearly demonstrated that transfected Alde-High EPCs had a wound repair ability that was similar to that of Alde-Low EPCs (necrotic area: PBS, 40.6% ± 8.2%; Alde-Low EPCs, 1.3% ± 2.3%; Alde-High EPCs, 39.0% ± 8.9%; Alde-High EPCs with MVs, 4.8% ± 6.3%; Fig. 6 A, B). Interestingly, HUVEC-transfected Alde-Low EPC-derived MVs showed less recovery from necrosis than the transfected Alde-High EPCs (data not shown).

Taken together, these results indicate that Alde-High EPCs possess a similar phenotype to Alde-Low EPCs from the point of the functional characteristics of EPCs in relation to neovascularization, suggesting that Alde-High EPCs would be a useful tool for investigating the molecular mechanisms underlying the angiogenic properties of Alde-Low EPCs.

2.2. HIF-2α, but not HIF-1α is a crucial factor for the expression of CXCR4 in EPCs

Our group previously found that under hypoxic conditions the expression of HIF-1α and HIF-2α were highly upregulated in Alde-Low EPCs in comparison to Alde-High EPCs [18]. To investigate the differences in the roles of these HIF factors in EPCs, the shRNAs of the HIFs were used to differentially decrease their expression. A western blotting analysis clearly showed that HIF-1α and HIF-2α were restrained by their respective shRNAs at levels of below 20% (Fig. 7 A, B). We subsequently examined the expression levels of the target genes of HIF-1α and HIF-2α in the HIF shRNA-treated cells after exposure to 1% O_2 for 6 h (Fig. 7C). VEGF mRNA expression was suppressed by both HIF-1α shRNA and HIF-2α shRNA [Alde-Low EPCs with HIF-1α shRNA, 0.51 ± 0.11-fold decrease, $P < 0.05$ ($n = 3$); Alde-Low EPC with HIF-2α shRNA, 0.23 ± 0.28-fold decrease, $P < 0.05$ ($n = 3$)]. Of note, CXCR4 mRNA expression was suppressed by HIF-2α shRNA, but not by HIF-1α shRNA [0.06 ± 0.03-fold decrease, $P < 0.01$ ($n = 3$)]. Collectively, the results indicate that HIF targeting genes are regulated differently by HIFs in EPCs and that further experiments are required to elucidate the mechanisms that underlie the differences in their regulation in EPCs.

To investigate how HIFs are involved in the functional role of Alde-Low EPCs *in vivo*, I analyzed the mouse model of skin flap ischemia. Seven days after the injection of Alde-Low EPCs into the tail vein, there was a reduction in the size of the

necrotic area (2.5% ± 5.3%, Fig. 8 A, B). However, Alde-Low EPCs with HIF-1α shRNA showed a reduced ability to repair the necrotic area [13.2% ± 2.81%, $P < 0.05$ ($n = 3$) vs. control Alde-Low EPC]. Remarkably, when Alde-Low EPCs with HIF-2α shRNA were injected, wound repair was significantly impaired and large necrotic areas were observed [34.1% ± 5.15%, $P < 0.01$ ($n = 4$) vs. control Alde-Low EPCs]. Further supporting this finding, a significantly lower number of GFP-labeled HIF-2α shRNA Alde-Low EPCs was detected at the site of the skin flap in comparison to mice that were injected with HIF-1α shRNA Alde-Low EPCs [control Alde-Low EPCs, 76.8 ± 5.9; Alde-Low EPCs with HIF-1α shRNA, 61.2 ± 4.6, $P < 0.05$ ($n = 3$); Alde-Low EPCs with HIF-2α shRNA, 13.5 ± 14.6 cells per field, $P < 0.01$ ($n = 3$), Fig. 8 C]. These results strongly suggest that CXCR4 is a crucial factor for cell migration and that in EPCs, the expression of CXCR4 is regulated by HIF-2α. Finally, we examined how the expression of CXCR4s is regulated in EPCs by HIF-2α using a chromatin immunoprecipitation (CHIP) assay. The CHIP assay clearly demonstrated that HIF-2α, but not HIF-1α binds to CXCR4 promoter region, indicating that HIF-2α is a key factor in the regulation of CXCR4 expression in Alde-Low EPCs (Fig. 8 D). HIF-1α may also be involved in the migratory activity of EPCs; however, the effect was less than that of HIF-2α, which suggests the possible existence of a separate mechanism that is related to EPC migration from the CXCR4/SDF-1 axis.

2.3. CXCR4 is a crucial factor in the migration of EPCs

I found that CXCR4 expression is profoundly regulated by HIF-2α, whereas VEGF expression is regulated by both HIF-1α and HIF-2α in Alde-Low EPCs. I next investigated the functional associations of CXCR4 and VEGF with the repair of ischemic tissue in the mouse model of skin flap ischemia. Alde-Low EPCs with CXCR4 shRNA or VEGF shRNA were prepared and used to examine the involvement of these genes in EPC migration.

CXCR4 mRNA expression in Alde-Low EPCs with CXCR4 shRNA showed a 0.25 ± 0.01-fold decrease [$P < 0.01$ ($n = 3$)] in comparison to the control under normoxic conditions [1.00 ± 0.59-fold ($n = 3$)] and a 0.33 ± 0.01-fold decrease [$P < 0.01$ ($n = 3$)] under hypoxic conditions [control: 2.39 ± 0.43-fold ($n = 3$)]. On the other hand, VEGF mRNA expression in Alde-Low EPCs with VEGF shRNA showed a 0.37 ± 0.09-fold decrease [$P < 0.01$ ($n = 3$)] in comparison to the control under normoxic conditions [control: 1.00 ± 0.30-fold, ($n = 3$)] and a 1.55 ± 0.18-fold decrease [$P < 0.01$ ($n = 3$)] under hypoxic conditions [control: 3.82 ± 0.37-fold, ($n = 3$)] (Fig. 9). The expression levels of the other HIFs target genes (Glut-1 and KDR) in the Alde-Low EPCs with these CXCR4/VEGF shRNAs did not differ from the control.

I then investigated the involvement of these genes in the repair of ischemic tissue in our mouse model of skin flap ischemia. Alde-low EPCs that were transfected with CXCR4 shRNA totally lost their ability to repair the ischemic sites.

In contrast, Alde-low EPCs that were transfected with VEGF shRNA showed a slight suppression in their ability to repair ischemic tissue [necrotic area: control Alde-Low EPCs, 3.0% ± 5.1%; Alde-Low EPCs with VEGF shRNA, 21.2% ± 9.1%; Alde-Low EPCs with CXCR4 shRNA, 35.5% ± 3.5% ($n = 3$ in each)] (Fig. 10 A, B).

CXCR4 is a chemokine receptor that is strongly associated with the migration of stem cells, including EPCs. To analyze the involvement of CXCR4 in the migration of EPCs, I performed two assessments. First, the number of migrated cells at ischemic sites was assessed in response to Alde-Low EPCs with GFP transfected with each shRNA (Fig. 10 C). I observed a 75% reduction in the number of GFP-positive cells following the injection of Alde-low EPCs with CXCR4 shRNA in comparison to the control [control Alde-Low EPCs, 76.8 ± 5.9 cells per field; Alde-Low EPCs with CXCR4 shRNA, 16.3 ± 10.3 cells per field, $P < 0.01$ ($n = 3$)]. When transfected with VEGF shRNA, the number of GFP-positive cells was not significantly different from that in the control Alde-Low EPCs [control Alde-Low EPCs, 76.8 ± 5.9 cells per field; Alde-Low EPCs with VEGF shRNA, 61.1 ± 7.2 cells per field ($n = 3$)].

Second, I performed an *in vitro* cell migration assay, which clearly showed that the migratory ability of Alde-Low EPCs was suppressed under hypoxic conditions in the presence of SDF-1 in the EPCs that were transfected with CXCR4 shRNA in comparison to the control Alde-Low EPCs [control Alde-Low EPCs: 2.95 ± 0.57 vs. Alde-Low EPCs with CXCR4 shRNA: 0.81 ± 0.28-fold, $P < 0.01$

($n = 4$); Fig. 10 D].

Collectively, these data demonstrated that the expression of CXCR4 was a crucial factor in the successful repair of ischemic tissue by Alde-Low EPCs in this model. Taken together, the results indicate that the CXCR4/SDF-1 axis promoted the migration of EPCs to the ischemic tissue in our mouse model of skin flap ischemia.

2.4. The effects of CXCR4 and VEGF gene overexpression in Alde-High EPCs

I subsequently examined whether the capacity of Alde-High EPCs to regenerate ischemic tissue was improved after the transfection of CXCR4 or VEGF genes. Alde-High EPCs are useful for determining the key molecules that play a functional role in Alde-Low EPCs in wound repair.

A reverse transcription-polymerase chain reaction (RT-PCR) clearly demonstrated the successful transfection of the target genes in Alde-High EPCs [CXCR4 overexpression: 18.6 ± 3.1-fold expression ($n = 3$); VEGF overexpression: 16.4 ± 2.0-fold expression ($n = 3$); Fig. 11]. An *in vitro* migration assay demonstrated that Alde-High EPCs, which were transfected with CXCR4, had a migratory ability that was similar to that of Alde-Low EPCs in the presence of SDF-1 under 5% O_2 conditions [Alde-Low EPCs, 2.95 ± 0.57-fold; Alde-High EPCs, 0.82 ± 0.18-fold; Alde-High EPCs with CXCR4 overexpression, 2.52 ± 0.41-fold ($n = 3$); Fig. 12 A].

I then examined whether CXCR4 and VEGF-transfected Alde-High EPCs possessed the wound repair ability in our mouse model of skin flap ischemia. The sizes of the necrotic areas expressed as a percentage of the total flap area were as follows:

3.0% ± 5.1%, 38.9% ± 2.1% in Alde-High EPCs, 13.1% ± 5.1% in the Alde-High EPCs with CXCR4 gene transfection ($P < 0.01$ vs. Alde-High EPCs), and 21.4% ± 9.1% in the Alde-High EPCs with VEGF gene transfection (Fig. 12 B, C; $n = 3$). These results clearly indicate that even when CXCR4 is expressed in Alde-High EPCs, their capacity to repair the ischemic tissue was still inferior to that in Alde-Low EPCs.

When I analyzed the number of transfected cells that were present at the site of the skin flap, I found that there were significantly more CXCR4-expressing Alde-High EPCs than there were normal Alde-High EPCs. However, the number of migrated CXCR4-expressing Alde-High EPCs was still lower than the number of Alde-Low EPCs [Alde-Low EPCs, 76.8 ± 5.9; Alde-High EPC, 11.3 ± 10.9; CXCR4-expressing Alde-High EPCs, 31.8 ± 9.4 cells per field, $P < 0.05$ ($n = 3$); (Fig. 12 D). These results indicate that the migratory effect related to CXCR4 was not sufficient to achieve the repair of the ischemic site, suggesting that there may be other factors involved in the wound repair ability of Alde-Low EPCs.

3. Discussion

EPCs that are harvested according to their cell surface markers show a hierarchy that is related to their growth activity [62]. Our group previously demonstrated that EPCs could be further separated into Alde-Low EPCs and Alde-High EPCs based on their ALDH activity [18]. The ability of Alde-Low EPCs to repair ischemic tissue is superior to that of Alde-High EPCs; however, the molecular

mechanisms that prove these differences have not been elucidated. To characterize the differentiating states of each type of EPCs, I transfected Alde-High EPCs with MVs isolated from Alde-Low EPCs. As expected, the wounds in the mouse model of skin flap ischemia showed a full recovery after treatment with Alde-High EPCs that were transfected with MVs derived from Alde-Low EPCs. This finding suggests that the differentiating states of Alde-Low EPCs and Alde-High EPCs are highly similar and that the comparison of these EPCs would enable me to investigate the molecular mechanisms that underlie their association with recovery from ischemia.

It has been reported that the direct intravenous injection of MVs derived from EPCs can improve revascularization after ischemic damage in a mouse model of hindlimb ischemia [63]. I also injected MVs (derived from Alde-Low EPCs) alone into the tail vein in a mouse model of skin flap ischemia. After treatment, however, the necrotic area did not significantly differ to that in the untreated control mice (data not shown). I cannot rule out the possibility that MVs alone are ineffective in repairing ischemic tissue, possibly because of the distance of the injection site from the site of skin flap. Further detailed analyses will be necessary to confirm the effectiveness of MVs by using a different ischemic model or a different transplantation method. In addition, it is speculated that the molecular composition of MVs derived from EPCs might change according to the physiological state. Indeed, the production of MVs was found to be enhanced after appropriate stimulation: in EPCs, hypoxia enhanced the production of MVs carrying miR-126 and miR-296

[64]. In this study, I investigated the effects of MVs released from Alde-Low EPCs under normal culture conditions. The results observed with MVs derived from Alde-Low EPCs might have been different in association with neovessel formation or angiogenesis regulated by miRNA functions or others [65, 66], if I harvested MVs from EPCs cultured under different conditions.

As described above, one of the key functions of EPCs *in vivo* is related to environmental stimuli, such as hypoxia. Under hypoxic conditions, EPCs, which are derived from the bone marrow, migrate through the peripheral blood to the sites of ischemia, where EPCs promote or directly contribute to the formation of new vessels [67, 68, 69]. Hypoxia-inducible factors, HIF-1α and HIF-2α, are known to respond to hypoxia, to form a heterodimer with Arnt and to transactivate the target genes [70]. It has been reported that these factors do not replenish each function, as shown by a knockout mouse study, and that the functional roles of these two factors are not fully understood [71]. In the present study, I found that HIF-1α and HIF-2α were both important in the transactivation of VEGF, whereas CXCR4 expression was profoundly regulated by HIF-2α in Alde-Low EPCs. Thus, the ability of Alde-Low EPCs that were transfected with HIF-2α shRNA to repair ischemic tissue was clearly reduced. Consequently, the size of the necrotic area was increased in comparison to the mice that were transfected with Alde-Low EPCs with HIF-1α shRNA. In fact, it has been shown that the expression level of SDF-1 that is secreted at the site of the skin flap is dependent on a low concentration of oxygen [34]. I also found that a high

level of SDF-1 was expressed in Alde-High EPCs plus MVs derived from Alde-Low EPCs. It suggests that in addition to inflammatory cells, SDF-1 receptor, CXCR4-expressing EPCs would be the first candidate cells to be recruited to the ischemic sites in our mouse model of skin flap ischemia. Alternatively, the CXCR4/SDF-1 axis might have survival/antiapoptotic effects on EPCs that enhance their engrafting capability in an autocrine manner [54].

Our group previously found that Alde-Low EPCs were incorporated into newly formed neovessels, indicating that transplanted EPCs contribute to the revascularization of ischemic tissue at the site of the skin flap rather than through the promotion of neoangiogenesis [18]. In the case of MSCs, we reported that, in addition to Alde-Low EPCs, transplanted AT-MSCs effectively repaired the perfusion of the blood flow in a mouse model of hindlimb ischemia, indicating that AT-MSCs promoted neoangiogenesis through a paracrine mechanism [58]. The migrated EPCs can secrete SDF-1 themselves to recruit the additional migration of CXCR4-positive EPCs or inflammatory cells to the site of ischemic tissues, suggesting that transplanted and migrated EPCs may function through a paracrine mechanism.

Taken together, these results indicate that while both HIF-1α and HIF-2α have an important role in the recovery from ischemia, the role of HIF-2α in association with EPCs would be crucial during the process of ischemic tissue repair. Importantly, in the present study, I did not observe similar or increased numbers of migrated EPCs

at the site of the ischemic skin flap, even when CXCR4 or VEGF were overexpressed in the Alde-High EPCs. Nevertheless, the ischemic tissue fully recovered after the transplantation of the control Alde-Low EPCs or the MV-transfected Alde-High EPCs. Deregibus *et al.* described the contribution of MV-derived antiapoptotic protein Bcl-xL in target ECs [38], and hypothesized that an antiapoptotic mechanism would be involved in the migration of EPCs and in their survival at the site of ischemia.

Chapter IV. Microvesicles derived from Alde-Low EPCs support wound healing ability of AT-MSCs

1. Purpose

Stem cell-derived Microvesicles (MVs) are capable of carrying functional RNAs and proteins to target cells through the way of horizontal transfer. Alde-Low EPCs are known to be suitable for the treatment of ischemic tissue. Interestingly, the transfection of MVs derived from Alde-Low EPCs to non-functional Alde-High EPCs results in gain of function on wound repair.

Mesenchymal stem cells (MSCs) are defined as multi-potent cells that can give rise to various kinds of differentiated cells, therefore thought to be useful for clinical therapy.

The aim of this study was to evaluate whether MVs released from Alde-Low EPCs exert a homing effect of AT-MSCs in a mouse model of wound healing. Moreover, I studied which molecules are associated with the wound healing process in MV-transfected AT-MSCs.

2. Results

2.1. Isolation of MVs derived from Alde-Low EPCs

I have shown that MVs derived from Alde-Low EPCs have capacity to change the properties of Alde-High EPCs for healing the wound [54]. To investigate whether the effect of MVs derived from Alde-Low EPCs is applicable in other cell type, we performed transfection of MVs into AT-MSCs that have not shown the wound healing ability when AT-MSCs are injected intravenously in the mouse flap model.

MVs were harvested from supernatant of Alde-Low EPCs culture by ultracentrifugation as described before [54], then isolated with cell sorter on the basis of surface markers for EPCs ($CD31^+$, $CD105^+$, $CD45^-$) (Fig. 13A). It has been reported that MVs are released from the cell surface and are capable of transferring mRNAs and proteins to other cells [54, 72], therefore I evaluated Alde-Low EPCs derived MVs by characterizing mRNA that is known to be involved in cell migration and/or angiogenesis. As shown in Fig. 13B, most of mRNAs examined were expressed similarly as that of parent cell, Alde-Low EPCs, suggesting that the isolation of MVs succeeded (Fig. 13B). In order to investigate the characteristics of AT-MSCs after receiving Alde-Low EPCs derived MVs, I performed co-culture of AT-MSCs and PKH26-labeled Alde-Low EPC-derived MVs. As shown in Fig.14 A, MVs were successfully internalized to target cell membrane after 12 hours incubation. To enrich the efficacy of the MVs in the AT-MSCs, MVs-incorporated

AT-MSCs was purified with cell sorter on the basis of fluorescein for PKH26 (Fig. 14B), and used for further analysis.

2.2. Characterization of AT-MSCs after receiving Alde-Low EPC-derived MVs

I next examined whether AT-MSCs transfected with Alde-Low EPC-derived MVs still possess characteristics of AT-MSCs. Under the microscopic observation, fibroblast-like morphology of AT-MSCs was similar as that of MVs-transfected AT-MSCs (Fig. 15). The analysis of MSC-specific cell surface markers ($CD90^+$, $CD105^+$, $CD73^+$, $CD14^-$, $CD31^-$, $CD45^-$, $CD34^-$, $CD271^-$, HLA-DR^-) showed no differences between the control AT-MSCs and MVs-transfected AT-MSCs (Fig. 16) except CD34 expression. CD34 is a glycoprotein and known to be expressed on the surface of hematopoietic stem cells and immature state of endothelial cells. The CD34 expression was slightly elevated in MVs-AT-MSCs.

AT-MSCs are known to be multi-potent stem cells and able to differentiate into adipocytes, osteocytes and chondrocytes [58, 73, 74]. Thus, I next examined differentiation ability. As shown in Fig. 17, AT-MSCs transfected with MVs exhibited ability to differentiate adipocytes and osteocytes as similar as the control AT-MSCs.

2.3. MVs derived from Alde-Low EPC alter mRNA and miRNA expression of AT-MSCs

I then examined EPC and MSC related genes as well as miRNAs by real-time PCR. Previously I showed that chemokine receptor, CXCR4 and VEGF expression

was highly involved in the homing capacity of EPCs by intravenous injection [54]. As shown in Fig.18, the expression of CXCR4 chemokine receptor was significantly elevated in AT-MSCs transfected with MVs (4.4 ± 0.9 fold increase, $P < 0.01$, n=3). On the other hand, the expression level of SDF-1, a ligand of CXCR4 showed no difference after transfection of MVs. The expression of VEGF showed slight increase (2.0 ± 0.5 fold increase, $P < 0.05$, n=3), and the expression of KDR, a receptor for VEGF was upregulated (2.8 ± 1.0 fold increase, $P < 0.05$, n=3) in MVs-AT-MSCs. The mRNA expression of chemokine, CCL2 and CCL5 that play an important role to recruit inflammatory cells at the sites of wound [50], was not different, although another chemokine IL-6 showed significant elevation (2.8 ± 0.9 fold increase, $P < 0.05$, n=3) in MVs -AT-MSCs. The cell adhesion related genes play an important role to regulate the injected cells to reach to the target sites efficiently. The mRNA expression of adhesion molecules such as ColIV and VCAM-1, were neither different in MVs-AT-MSCs compared to the control. In addition, the mRNA expression of cell proliferation-related genes, such as TGF-β and b-FGF, were not different between them. Moreover, MVs contain miRNAs, which are small non-coding RNAs that function as guide molecules in RNA silencing and ~22 nucleotides in length [75]. In previous reports demonstrated that miR-126, miR-296 are regulated mobilization and migration of bone marrow-derived mononuclear cells as well as angiogenesis process [76, 77]. Chen *et al.* demonstrated that MSCs transfected with miR-126 survived a long time and effectively expressed miR-126 for at least six weeks at the injected area in myocardial infarction mouse model. The intra-myocardial injection of MSCs

overexpressing miR-126 into ischemic myocardium significantly enhanced the vessel density, resulting in the improvement of angiogenesis [76]. Consistent with these reports, I found that miR-126 and miR-296 were highly expressed in MV-transfected AT-MSCs compared with the control AT-MSCs ($P<0.01$, n=3 in each) (Figure 19).

Previously, I demonstrated that hypoxia inducible factors (HIFs), especially HIF-2α is highly expressed in Alde-Low EPCs and is responsible for cell migration toward the wound sites thorough the positive regulation of CXCR4 expression [54]. There was no significant difference of HIF-2α expression in MVs-AT-MCSs compared to the control at mRNA and protein levels (data not shown), suggesting the expression of CXCR4 in MVs transfected AT-MSCs is not depend on HIF-2α regulation.

Collectively, these data suggested that MVs derived from Alde-Low EPCs were capable to alter gene expression profile in AT-MSCs but different from the case of Alde-High EPCs and miRNAs shuttled by MVs contributed to AT-MSC's regenerative potential.

2.4. MVs derived from ALDH-Low EPCs enhance migration ability of AT-MSCs

It has been shown that AT-MSCs exhibited low cell migratory ability and only cure wound when injected at injured area directory [78]. I then investigated the capacity of AT-MSCs in wound healing while injecting directly to skin of ischemia model. As shown in Fig. 20, mouse flap model clearly showed that the area of

necrosis was smaller in the mice injected with AT-MSCs when comparing with mice injected PBS (necrotic area: control PBS: 59.8% ± 6.6%, AT-MSCs: 16.2% ± 9.5%). On the other hand, I have previously reported that CXCR4 is crucial factor for the migration of Alde-Low EPCs at the site of wound [54]. To characterize the functional role of AT-MSCs with MVs, I performed *in vitro* scratch assay that can mimic cell migration during wound healing [59]. As shown in Fig. 21A, *in vitro* scratch assay clearly showed higher migratory ability in MVs-transfected AT-MSCs compared to the control AT-MSCs (% migration distance: AT-MSCs with MVs-derived from Alde-Low EPCs, 402.0 % ± 51.2 %; control, 157.2 % ± 49.4 %; $P < 0.001$, n=3).

Then I investigated whether Alde-low EPC-derived MVs could effect on the proliferation activity in AT-MSCs. As shown in Fig. 21 B, no significant difference was observed in the cell growth between MVs transfected AT-MSCs and the control AT-MSCs.

Hence, these results suggested that AT-MSCs specifically acquired migration ability but not proliferation ability by MVs derived from Alde-Low EPCs.

2.5. AT-MSCs gained the ability to repair wound by transfection of MVs derived from Alde-Low EPCs

I next examined whether MVs-AT-MSCs possess the capacity to impair the wound healing process in the mouse flap model [54].

In order to assess migratory ability *in vivo*, I analyzed the localization of AT-MSCs at the wound sites after intravenous injection. As shown in Fig. 22A, 24 hours

later from the injection through tail vein, PHK67 (green fluorescent)-labeled AT-MSCs with MVs were detected at wound site whereas the control AT-MSCs were barely detected at the site. Subsequently, in order to verify whether inflammatory cells were recruited at the wound site following the AT-MSC arrival, the number of $CD45^+$ cells was scored on day 3 after the injection. As shown in Fig. 22 B, C, significantly higher number of $CD45^+$ cells were observed at the wound site in the MVs-AT-MSCs compared to the control AT-MSCs ($CD45^+$cell number/field: AT-MSCs, 28.7 ± 1.8; AT-MSCs with MVs-derived from Alde-Low EPCs, 40.1 ± 3.0, $P < 0.01$, n=3).

Moreover, *in vivo* wound healing efficiency was evaluated by measuring size of necrotic area on day 7 after the injection. As shown in Fig. 22D, AT-MSCs with MVs exhibited high capacity to repair the wound compared to the control AT-MSCs (necrotic area: control PBS: 72% ± 4.6%, Alde-Low EPCs: 9.7% ± 5.7%, AT-MSCs, 67.0% ± 0.1%; AT-MSCs with MVs-derived from Alde-Low EPCs, 10.4 % ± 8.6%, $P < 0.05$, n=3).

Collectively, these results indicate that MVs derived from Alde-Low EPCs are capable for changing the properties of AT-MSCs to possess the homing ability to migrate to the wound site *in vivo* (Fig. 23).

3. Discussion

Here, I show that MVs from EPCs derived from UCB provide an important potential as a therapeutic tool for AT-MSCs. Importantly, MVs possess the abilities to compensate and change the properties in the recipient cells by delivering their bioactive factors, therefore these effects could expand a novel therapeutic strategy.

Our group previously demonstrated that EPCs are subdevided into two populations based on their ALDH activity, such as Alde-Low and Alde-High EPCs [18]. In addition, we showed that Alde-Low EPCs efficiently repairs ischemic tissues because CXCR4 and VEGF are highly expressed under hypoxic conditions compared to Alde-High EPCs [18]. In fact, transfection of MVs isolated from Alde-Low EPCs was effective to change the properties of Alde-High EPCs to improve the wound healing process [54].

MSCs themselves are known to release MVs that mimic the beneficial effects of target cells, suggesting those MVs derived from MSCs may induce various kinds of regenerative functions of MSCs [79, 80].

In the present study, I performed transfection of MVs derived from Alde-Low EPCs into AT-MSCs. AT-MSCs that was originally unable to repair the wound when transplanted intravenously (Fig. 22D) became to migrate at the wound sites after the incorporation of MVs derived from Alde-Low EPCs. These facts suggested that the effect of MVs would be conserved and applicable to other type of stem cells other than AT-MSCs.

Consistent with previous reports, AT-MSCs are able to repair the wound when they are directly transplanted to the wound sites. Subsequently, AT-MSCs secrete chemokines (such as SDF1, CCL5) and $CD45^+$ inflammatory cells including monocytes and lymphocytes are recruited to promote the first step of wound healing [81]. Migration ability of AT-MSCs is defective in the wound healing process when intravenous transplantation was performed. In this study, I found there were no obvious differences on the expression levels for SDF-1 and CCL5 between the control AT-MSCs and MVs-transfected AT-MSCs (Fig. 18). Of note, significant upregulation of CXCR4 was observed in AT-MSCs with MVs derived from Alde-Low EPCs (Fig. 18). In accordance with the result, the migratory ability of AT-MSCs with MVs was also enhanced *in vitro* compared to the control (Fig. 21A). It has been reported that SDF-1 is secreted at the site of skin flap dependent on degree of low oxygen tension [34]. Thus, CXCR4 highly-expressed AT-MSCs may be attracted and migrated to the wound sites where the expression of SDF-1 is upregulated.

Gheisari *et al.* reported that CXCR4 and CXCR7, which is another SDF-1 receptor, were overexpressed in bone marrow MSCs, and those cells were injected in a mouse model of cisplatin-induced acute kidney injury. They found overexpression of CXCR4 and CXCR7 in BM-derived MSCs could not improve the homing and therapeutic potentials of those cells [82]. In contrast, other groups reported that autologus MSCs transplantation showed renoprotective effects [83]. These controversies might be explained by differences in the protocol of cell

transplantation, the animal strain, and type and severity of kidney injury. This study evokes one important mechanism on AT-MSCs homing in wound healing process, however it also suggests a measurement in the same conditions would be necessary to clarify the mechanism for clinical use of AT-MSCs.

It is well known that MSCs secrete various kinds of cytokines and growth factors. IL-6 is one of secreted factors from MSCs, and reported that inhibit lymphocyte apoptosis via direct interactions each other [84]. Pricola *et al.* have reported that IL-6 maintains the proliferative and undifferentiated states of bone marrow-derived MSCs. They also suggested that IL-6 has potency to protect bone marrow-derived MSCs from apoptosis and increases *in vitro* wound healing activity [84]. In the present study, significant increase of IL-6 expression was observed in AT-MSC transfected MVs derived from Alde-Low EPCs (Fig. 18), suggesting that upregulated expression of IL-6 in MVs-AT-MSCs might act in a paracrine fashion to impair the wound healing process.

It has been reported that MVs are capable of transferring not only mRNAs but also miRNAs to other cells [85, 86, 87]. Micro-RNAs are small noncoding RNA (~22 nucleotides) and known to be able to regulate the gene expression at a post-transcriptional level through the translational inhibition and/or destabilization of targeted mRNAs [88, 89]. Several lines of evidences have shown that miRNAs are involved in angiogenesis, cell survival and CXCR4 regulation in ischemic tissue. Thus, I examined expression of miRNAs in MVs-transfected AT-MSCs, and found

significant increase of miR-126, miR-296 (Fig. 19). Thus, it is conceivable that the improved wound healing with MVs-transfected AT-MSCs was achieved by several molecular mechanisms such as migration factors and miRNAs.

It is reported that appropriate stimulus such as hypoxia enhance the production of MVs carrying miR-126 and miR-296 from EPCs [90]. In this study, I investigated the effects of MVs released from Alde-Low EPCs without any stimulus. Thus, it may be intriguing issue to investigate a different effect of MVs derived from Alde-Low EPCs cultured in hypoxic condition.

Chapter V. Conclusion and Perspective

Conclusion

In my studies, I proved the crucial role of CXCR4 expressed on Alde-Low EPCs in the process of ischemic tissue repair. While CXCR4 is profoundly regulated by HIF-2α, another candidate gene, VEGF is regulated by HIF-1α and HIF-2α in Alde-Low EPCs. To specify the target molecules in each step of recovery from ischemia, further investigation will be needed to clarify the complicated mechanisms that underlie the tissue repair process. The precise analysis of the function of EPCs would provide new evidence that could be applied to stem cell therapy for patients with tissue ischemia of various etiologies.

Moreover, I provided the possibility that Alde-Low EPCs-derived MVs may be useful tool to change the properties of AT-MSCs into applicable for intravenous and/or intra-arterial injection treatment. I still do not know whether MVs derived from Alde-Low EPCs would be effective for the migration of other type of stem cells. Further studies would be necessary to prove the key molecules including CXCR4 associated with the homing of AT-MSCs as well as other type of MSCs. These results might bring therapeutic breakthrough for a difficult disease to treat, for example, long standing ulcers with dense scar tissue.

Perspective

Recently, a number of studies about EPCs are increasing due to function of EPCs in neovascularization. Moreover, EPCs can be applied to treat disease related to ischemia. It is required a specific marker to isolate functional EPCs. Our group reported that ALDH activity is a useful marker to isolate functional EPCs (Alde-Low EPCs) which show migration ability as well as facilitation wound healing in the mouse flap model. CXCR4, a chemokine receptor which is directly regulated by HIF-2α, plays important role in EPC migration ability to wound site. Knockdown of CXCR4 expression in Alde-Low EPCs impaired wound healing ability. Of note, cancer cells expressed high level of CXCR4 mRNA. Thus, understanding of CXCR4 function can support to control EPC therapy as well as contribute to study about cancer cell metastasis. The overexpression of CXCR4 in Alde-High EPCs (non-functional EPCs) improves their migration, resulting in wound healing. To enhance the effect of the improvement of migration ability, microvesicles derived from Alde-Low EPCs might be a good candidate to change characteristics of recipient cells. My data demonstrated that MVs derived from Alde-Low EPCs can improve migration of Alde-High EPCs and AT-MSCs by upregulated genes expression related to migration, angiogenesis, cell survival, adhesion and proliferation. Further examination of MVs function is needed to clarify the mechanism of genes delivery as well as tumorgenesis. Understanding of MVs function can build a foundation to other research fields such as cell biology, cancer cell and drug delivery.

Figures and legends

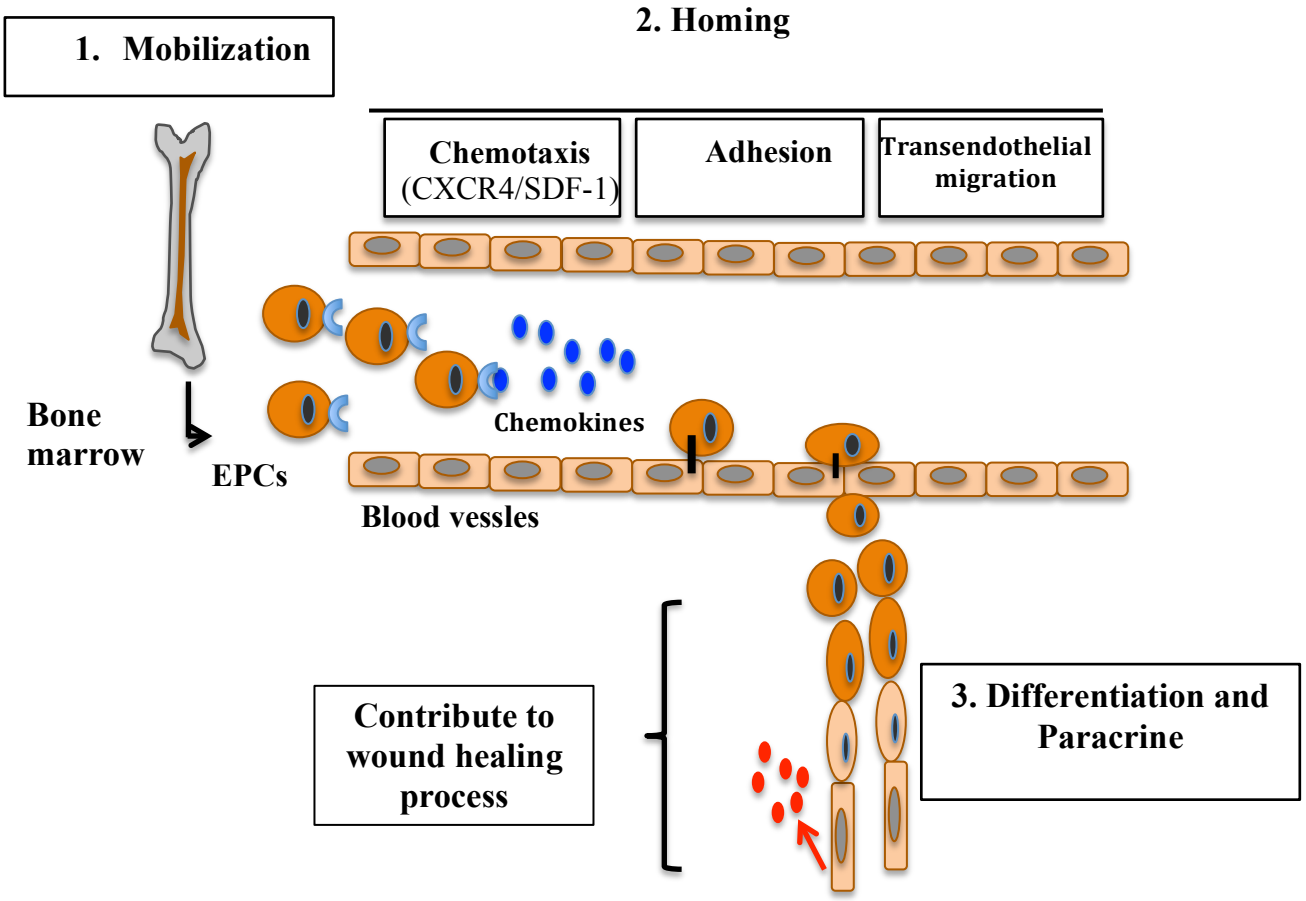

Figure 1. EPCs contribute to the repair of injured vessels

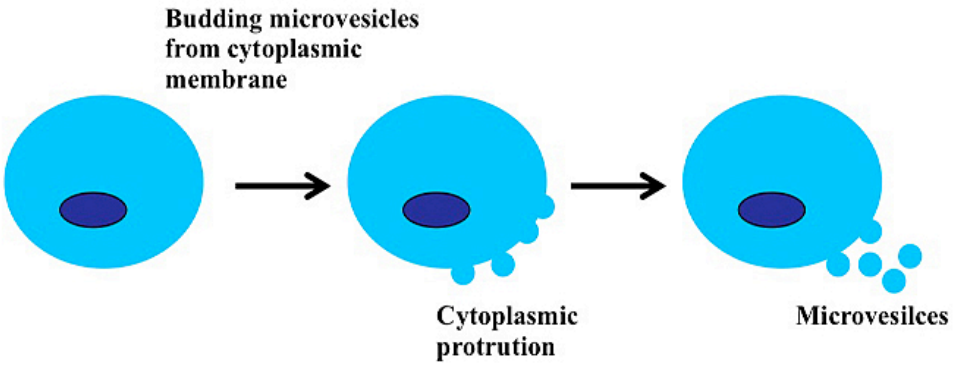

Figure 2. Microvesicle budding from cytoplasmic membrane.

Budding process takes place at unique locations on the cell membrane that are enriched with specific lipids, mRNAs, miRNAs and proteins reflecting their cellular origin.

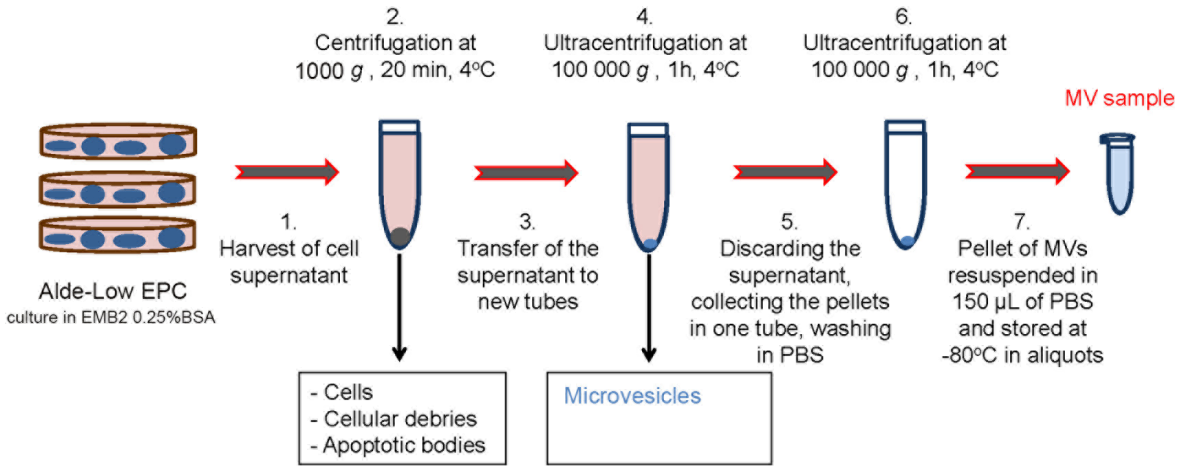

Figure 3. Isolation protocol of microvesicles

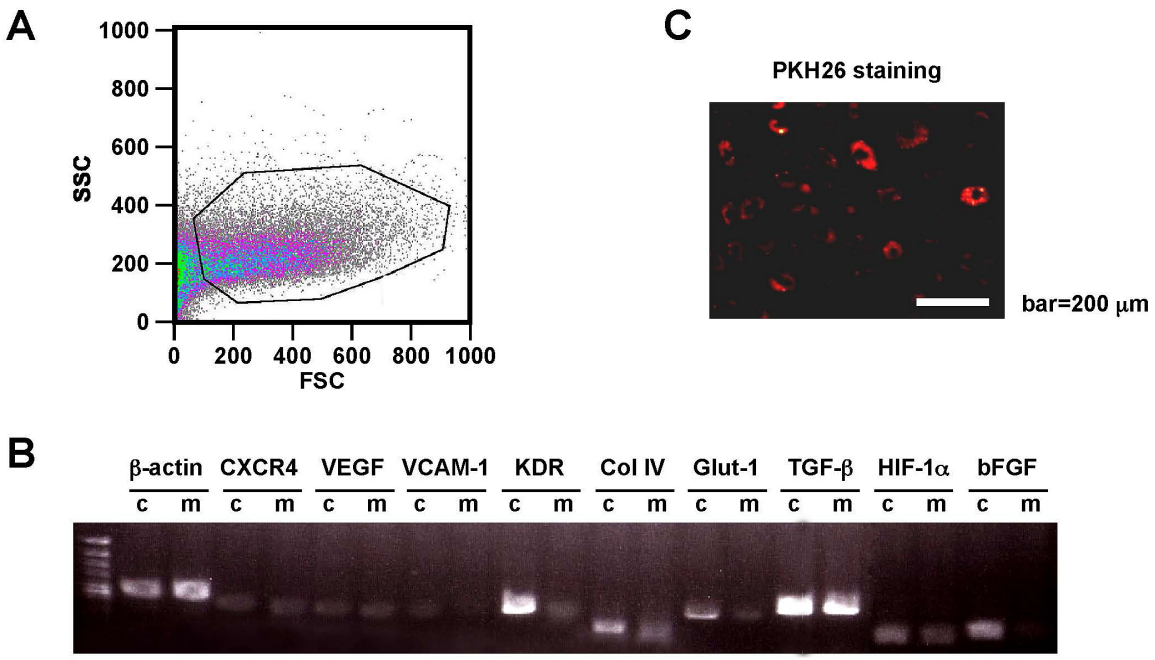

Figure 4. Characteristic of MVs derived from Alde-Low EPCs.

(A) MVs derived from Alde-Low EPCs were isolated by FACS after centrifugation. **(B)** The analysis of mRNA levels of the indicated genes in MVs and parental cells by an RT-PCR. c, Alde-Low EPCs; m, MVs derived from Alde-Low EPCs. **(C)** MVs derived from Alde-Low EPCs were stained with PKH-26 (red fluorescent) and transfected to cells. After 12 h, the cells were observed under fluorescence microscope. Scale bar: 200 μm.

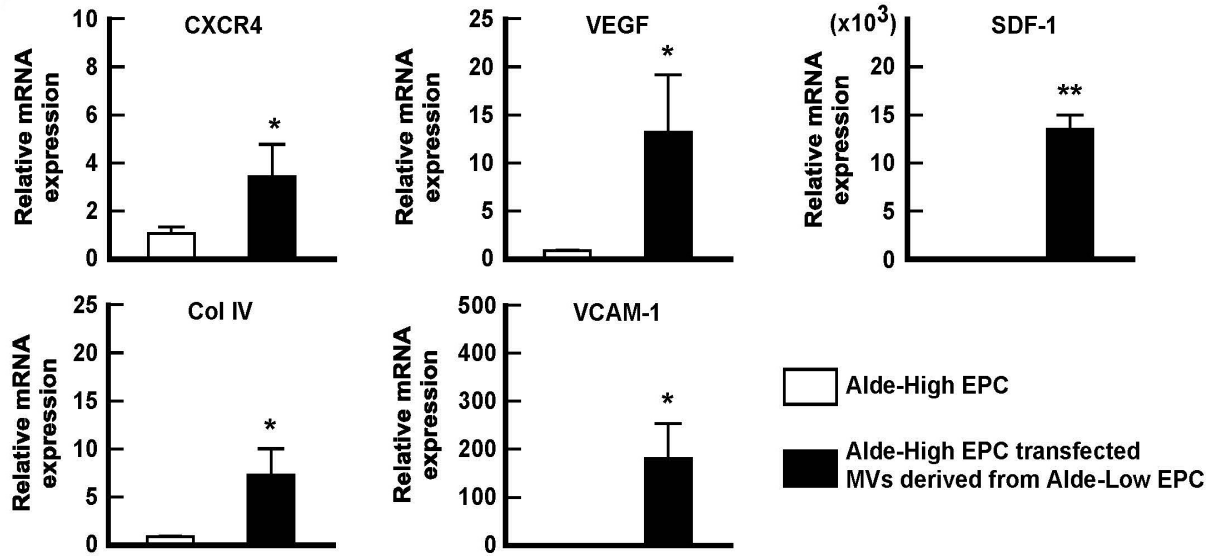

Figure 5. Angiogenic gene expression of Alde-High EPCs transfected MVs derived from Alde-Low EPCs

CXCR4, VEGF, SDF-1, ColIV, and VCAM-1 mRNA expression were analyzed in Alde-High EPCs that were transfected with MVs (*black bar*) in comparison to Alde-High EPCs (*white bar*) under normoxic conditions. The expression level detected in Alde-High EPCs was normalized to a value of 1 as the standard for each factor. *$P < 0.05$, **$P < 0.01$.

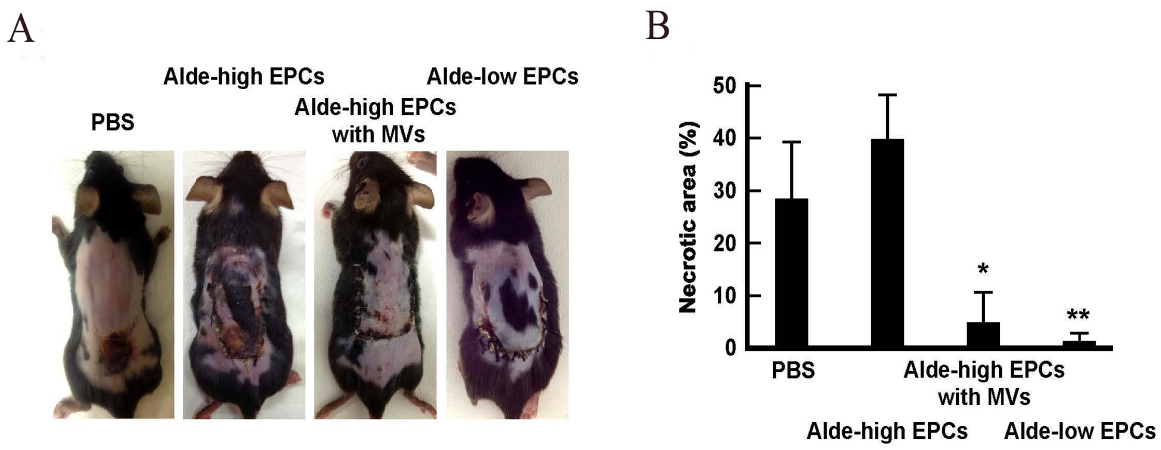

Figure 6. MVs derived from Alde-Low EPCs can improve the *in vivo* angiogenic activity of Alde-High EPCs

(A) Skin incisions were created on the dorsal skin of mice. PBS alone, Alde-Low EPCs, Alde-High EPCs, or Alde-High EPCs with MVs were injected to the mice. The effects of the EPCs in the recovery from ischemia were analyzed on day 7 after surgery. **(B)** The necrotic regions in the four different types of mice ($n = 3$ in each) were measured. Note that the area of necrosis in the mice that were injected with Alde-High EPCs with MVs was similar to that in mice that were injected with Alde-Low EPCs. *$P < 0.05$, **$P < 0.01$.

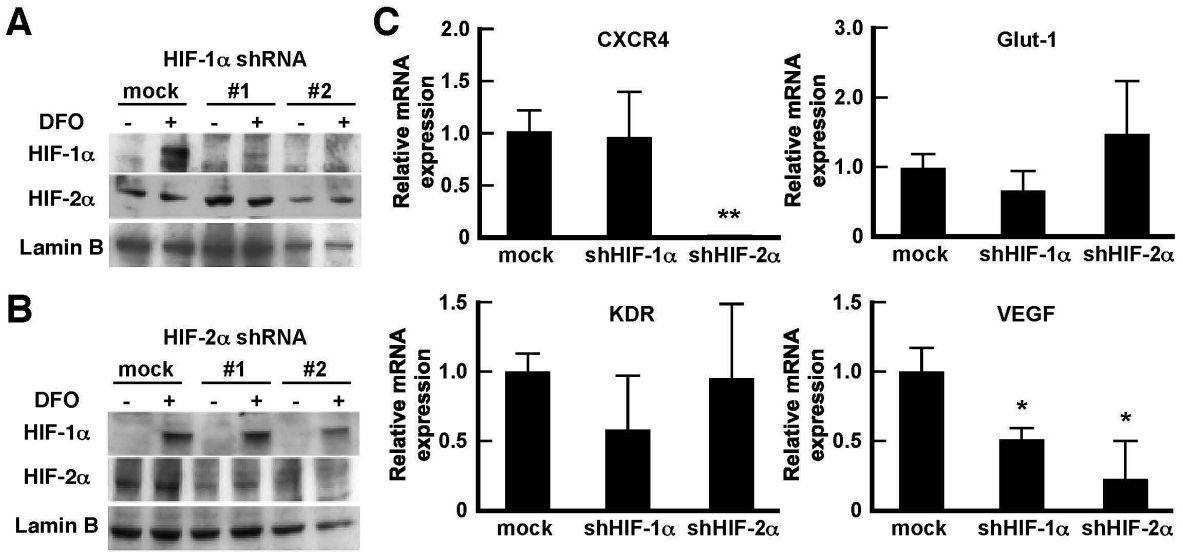

Figure 7. Analysis of the involvement of HIF-1α and HIF-2α in the repair of ischemic tissue of Alde-Low EPCs shRNA HIFs.

(A, B) The protein expression levels of HIF-1α **(A)** and HIF-2α **(B)** were analyzed by western blotting in mock Alde-Low EPCs (control), Alde-Low EPCs transfected with shHIF-1α RNA, or Alde-Low EPCs transfected with shHIF-2α RNA. The control cells and the two types of transfected cells (#1 and #2) were treated with (+) or without (−) 100 μM DFO for 6 h before the analysis. **(C)** The mRNA expression level of the indicated genes in the Alde-Low EPCs, the Alde-Low EPCs with HIF-1α shRNA, and the Alde-Low EPCs with HIF-2α shRNA were measured using an RT-PCR. Note that the CXCR4 expression was downregulated by HIF-2α shRNA, but not by HIF-1α shRNA. *$P < 0.05$, **$P < 0.01$.

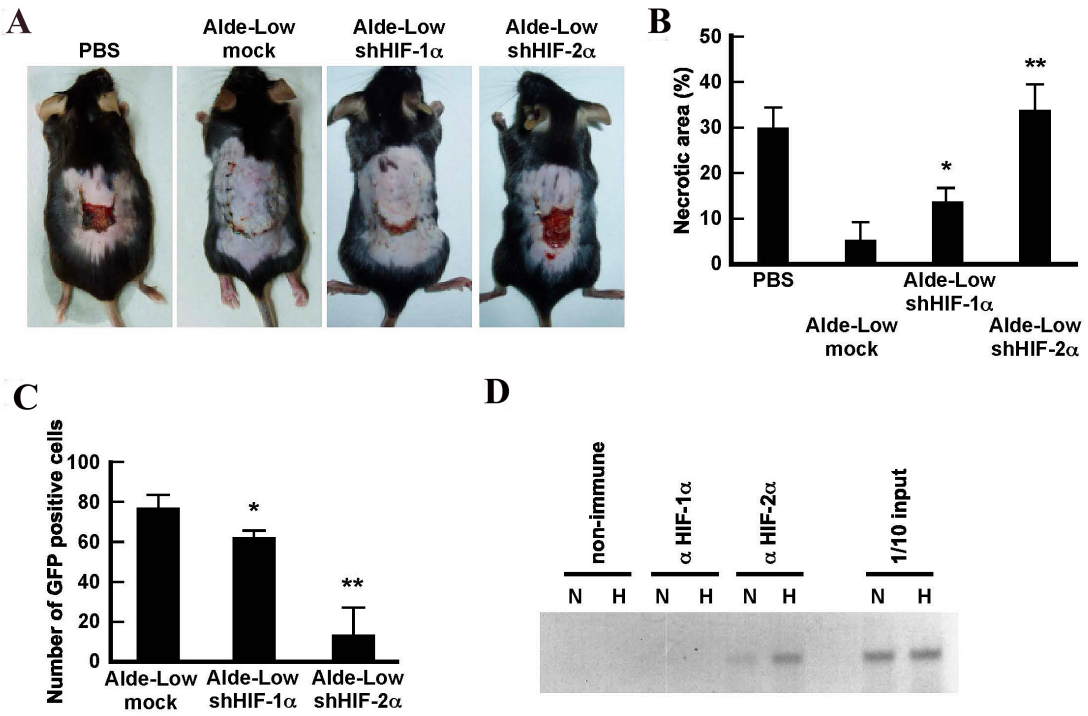

Figure 8. The involvement of HIF-1α and HIF-2α in *in vivo* angiogenesis ability of Alde-Low EPCs shRNA HIFs

(A) Skin incisions were created on the dorsal skin of mice. PBS, mock Alde-Low EPCs, Alde-Low EPCs with HIF-1α shRNA, or Alde-Low EPCs with HIF-2α shRNA were injected into the mice. The effects of the EPCs on the repair of ischemic tissue were analyzed on day 7 after surgery. **(B)** The necrotic regions in the four types of mice ($n = 3$ in each) were measured. Note that in the ability to repair ischemic tissue was lost in mice that were injected with Alde-Low EPCs with HIF-2α shRNA. *$P < 0.05$, ** $P < 0.01$.

(C) The number of migrated GFP^+ cells was measured. Note that the number of GFP^+ cells at the site of skin flap was decreased in the mice that were injected with Alde-Low EPCs with HIF-2α shRNA. *$P < 0.05$, **$P < 0.01$.

(D) A CHIP assay was performed to examine binding to the hypoxia response element (HRE) region of the CXCR4 promoter under normoxic (N) and hypoxic conditions (H). Note that HIF-2α, but not HIF-1α, binds to CXCR4 promoter under both conditions. CHIP, chromatin immunoprecipitation; DFO, desferrioxamine; GFP, green fluorescent protein; HIF, hypoxia-inducible factor; shRNA, short hairpin RNA.

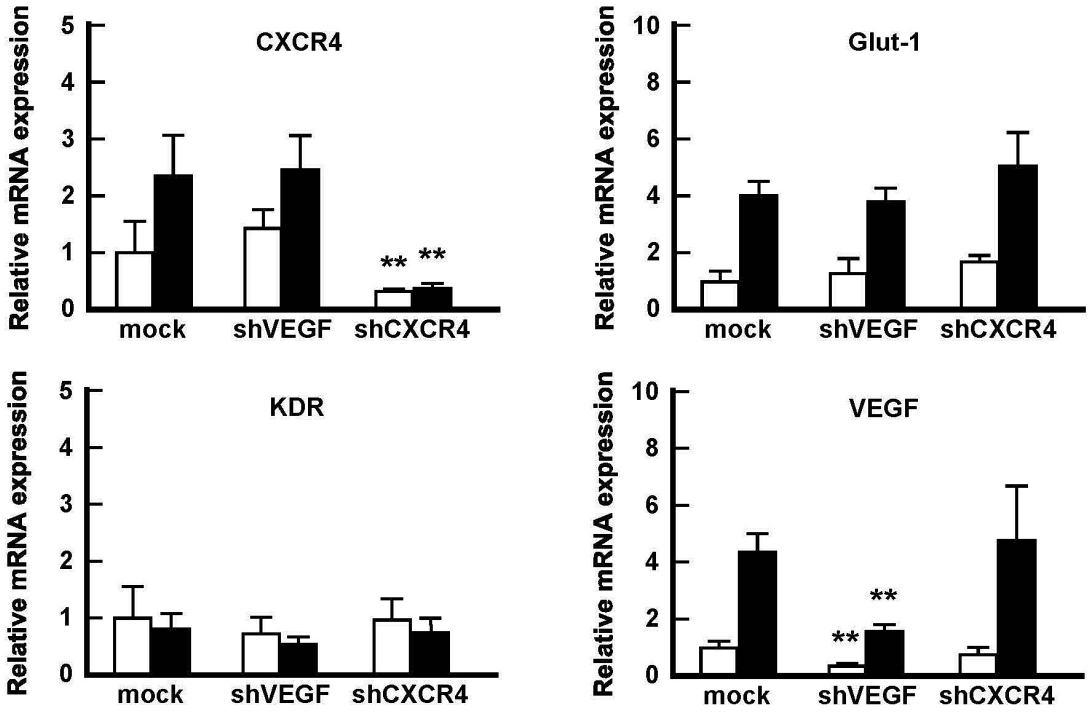

Figure 9. Analysis of the expression of CXCR4 and VEGF genes in Alde-Low EPCs shRNA CXCR4 or VEGF

The mRNA expression levels of the indicated genes in mock Alde-Low EPCs, Alde-Low EPCs with VEGF shRNA, or Alde-Low EPCs with CXCR4 shRNA were analyzed by a qPCR [*white bar*: normoxic conditions; *black bar*: hypoxic conditions (1% O_2 for 6 h)]. The expression levels that were detected in the mock Alde-Low EPCs under normoxic conditions were normalized to a value of 1 as the standard for each gene. $^{**}P < 0.01$.

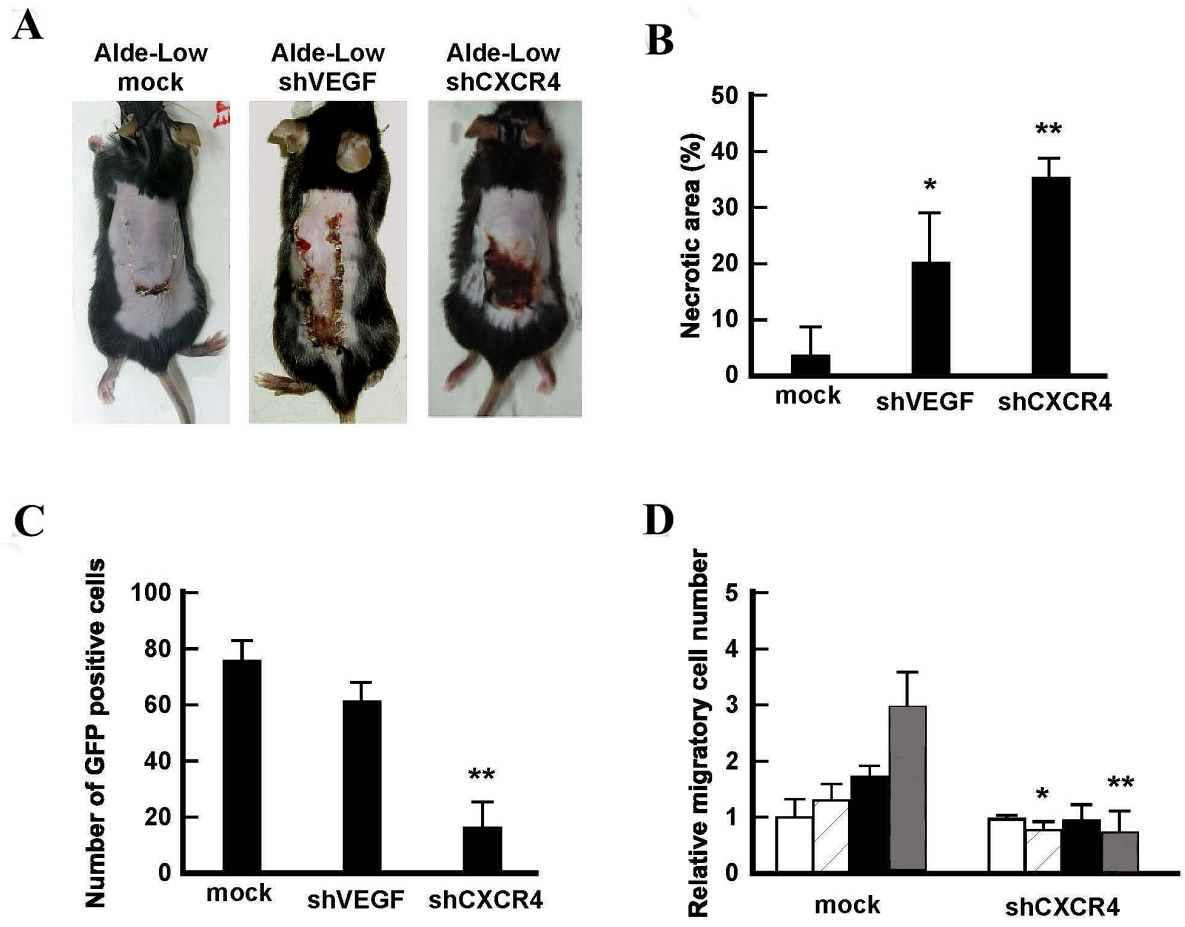

Figure 10. Analysis of the involvement of CXCR4 and VEGF in the repair of ischemic tissues of Alde-Low EPCs knockdown CXCR4 or VEGF genes.

(A) Skin incisions were created on the dorsal skin of mice. Mock Alde-Low EPCs, Alde-Low EPCs with VEGF shRNA, or Alde-Low EPCs with CXCR4 shRNA were injected into the mice. The effect of EPCs on the repair of ischemic tissue was analyzed on day 7 after surgery. **(B)** The necrotic regions in the mice that were injected with three different types of EPCs ($n = 3$ in each) were measured. *$P < 0.05$, **$P < 0.01$.

(C) The number of migrated GFP-labeled Alde-Low EPCs at the site of the skin flap was counted. ***P < 0.01*. **(D)** An *in vitro* transwell culture assay was performed to analyze *in vitro* migration. The migratory ability of Alde-Low EPCs with CXCR4 shRNA was analyzed and compared with that of the mock Alde-Low EPCs in the presence of SDF-1. *White bar*, 20% O_2 without SDF-1; *white striped bar*, 20% O_2 with SDF-1; *black solid bar*, 5% O_2 without SDF-1; *gray bar*, 5% O_2 with SDF-1. **P < 0.05, **P < 0.01*. qPCR, quantitative PCR.

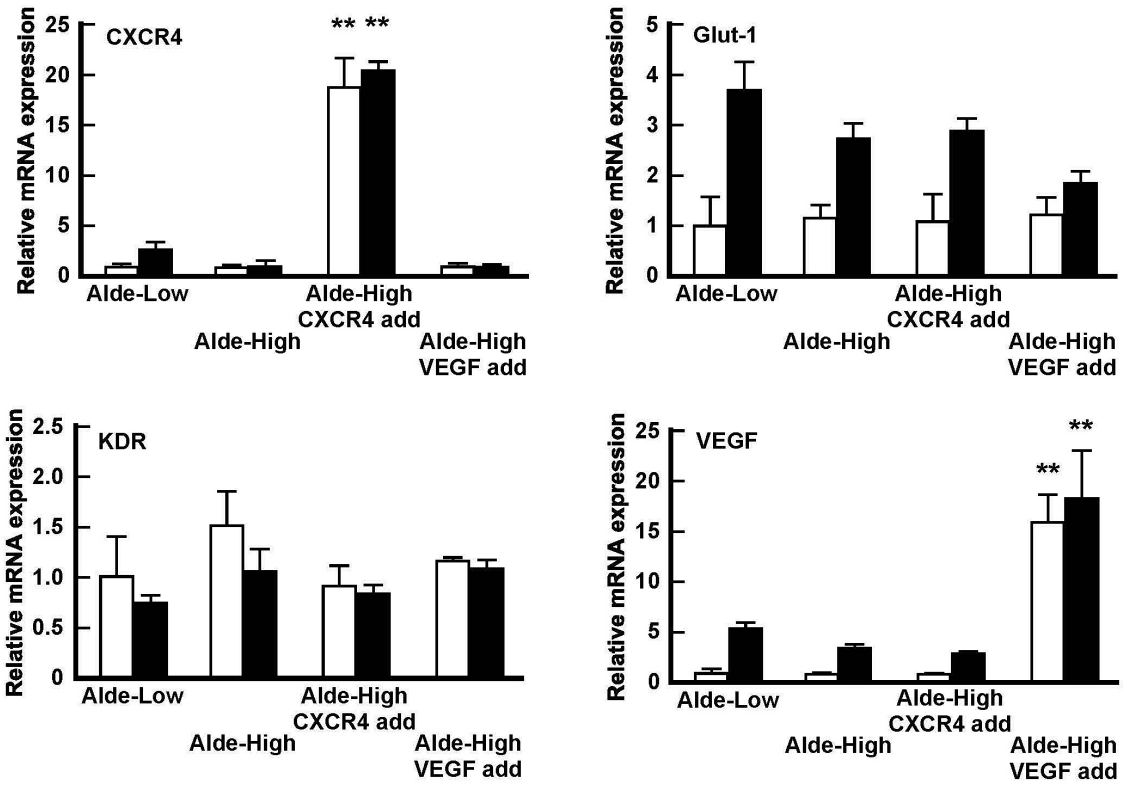

Figure 11. Analysis of angiogenic gene expression of Alde-High EPCs with CXCR4 or VEGF overexpression.

The mRNA expression levels of the indicated genes in mock Alde-Low EPCs (control), mock Alde-High EPCs (control), Alde-High EPCs-CXCR4 overexpression, and Alde-High EPCs-VEGF overexpression were analyzed using a qPCR [*white bar*: normoxic conditions; *black bar*: hypoxic conditions (1% O_2 for 6 h)]. The expression level of the mock Alde-Low EPCs under normoxic conditions was normalized to a value of 1 as the standard for each gene. ***P < 0.01*.

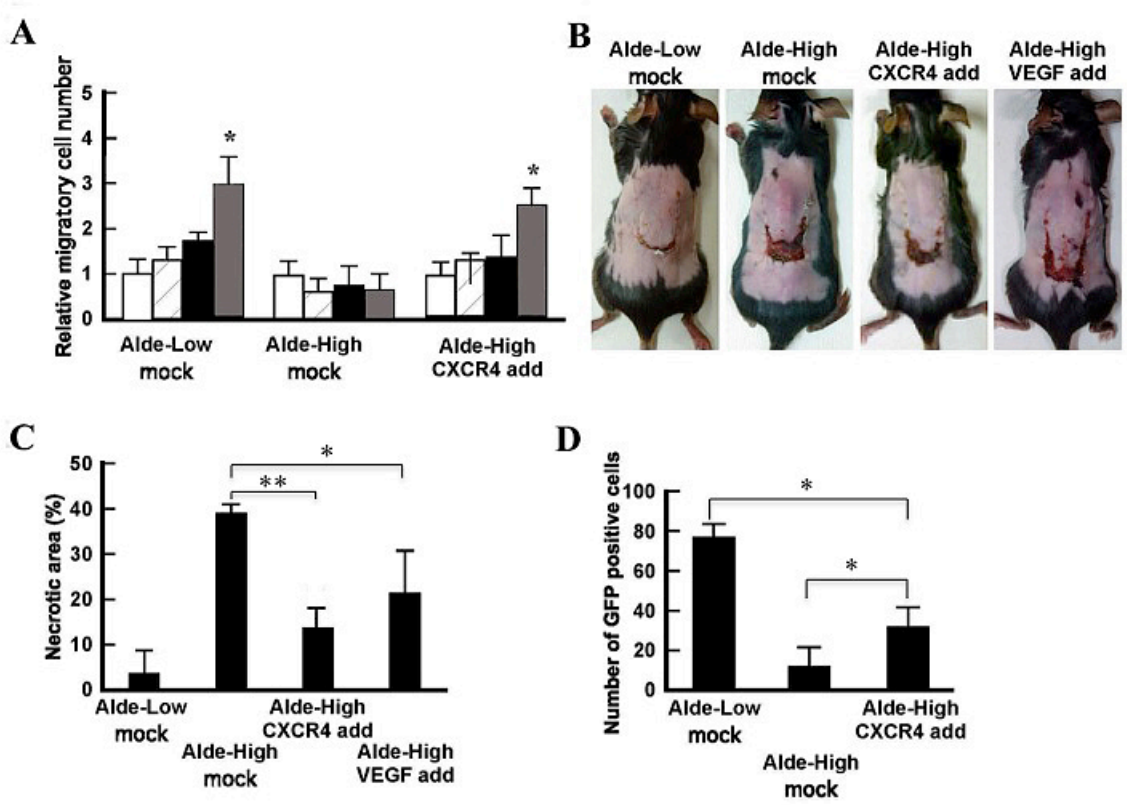

Figure 12. Wound healing *in vitro* and *in vivo* in Alde-High EPCs transfected CXCR4 or VEGF genes

(A) The migration ability of EPCs was analyzed with an *in vitro* transwell culture assay. The migratory ability of Alde-Low-EPCs (positive control), mock Alde-High EPCs, or Alde-High EPCs with CXCR4 overexpression in the presence of SDF-1 was investigated. *White bar*, 20% O_2 without SDF-1; *striped bar*, 20% O_2 with SDF-1; *black bar*, 5% O_2 without SDF-1; *gray bar*, 5% O_2 with SDF-1. *$P < 0.05$.

(B) Skin incisions were created on the dorsal skin. Alde-Low EPCs, mock Alde-High EPCs, Alde-High EPCs with CXCR4 overexpression, or Alde-Low EPCs with VEGF

overexpression were injected into the mice. The effects of EPCs on the repair of ischemic tissue were analyzed on day 7 after surgery.

(C) The necrotic regions in the four types of mice ($n = 3$, each) were measured. Note that the recovery of ischemic tissue was superior in mice that were injected with Alde-High EPCs with CXCR4 overexpression to that in mice that were injected with Alde-High EPCs. *$P < 0.05$, **$P < 0.01$. **(D)** The number of migrated cells at the site of the skin flap was measured. Note the difference in the number of migrated cells in the mice that were injected with Alde-High EPCs with CXCR4 overexpression and the mice that were injected with Alde-Low EPCs. *$P < 0.05$.

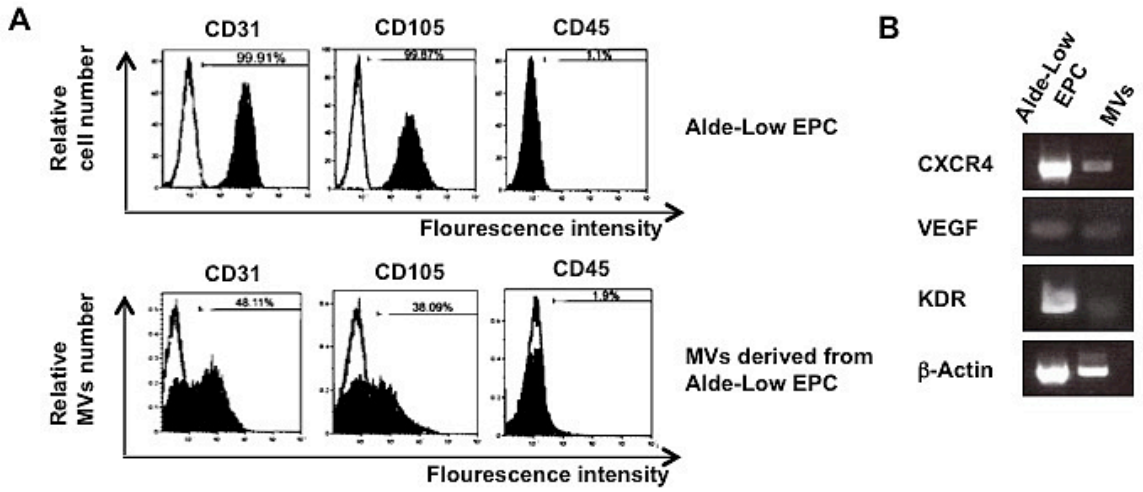

Figure 13. Characteristics of specific cell surface marker and gene expression of MVs derived from Alde-Low EPCs.

(**A)**. Representative FACS analysis of the Alde-Low EPCs and their MVs at 37°C. MVs derived from Alde-Low EPC are positive for CD31, CD105 and negative for CD45. (**B)**. Analysis of mRNA levels for some selected genes in MVs and parental cells. All transcripts were analyzed using real-time polymerase chain reaction (PCR). PCR products were visualized on 2% agarose gel.

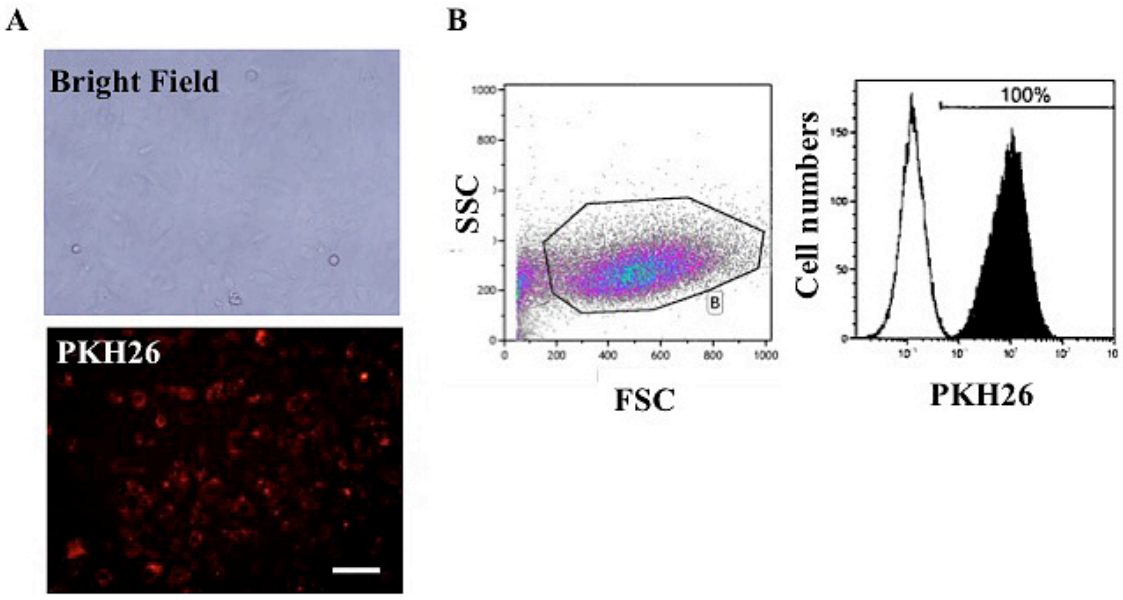

Figure 14. Characteristics of the internalize ability of MVs derived from Alde-Low EPCs.

(A). Alde-Low EPCs derived MVs were stained by PKH26 (Red fluorescent –Sigma) and transfected to AT-MSCs. After 12 h of incubation, cells were visual under fluorescent microscope. Bar indicates 200 μm. **(B)**. FACS analysis of red fluorescent in transfected cells.

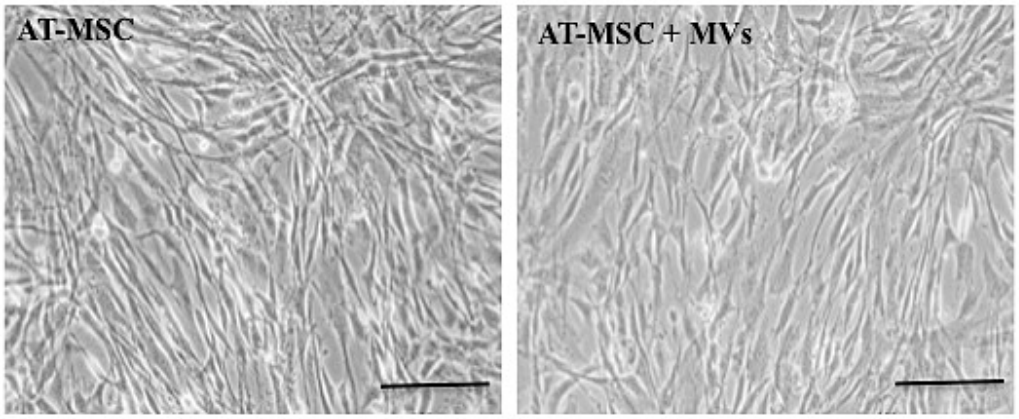

Figure 15. Comparison of morphology between AT-MSCs and AT-MSCs transfected MVs derived from Alde-Low EPCs

AT-MSCs and AT-MSCs transfected MVs showed the spindle-shaped and fibroblast-like morphology. Scale bar indicates 200 μm.

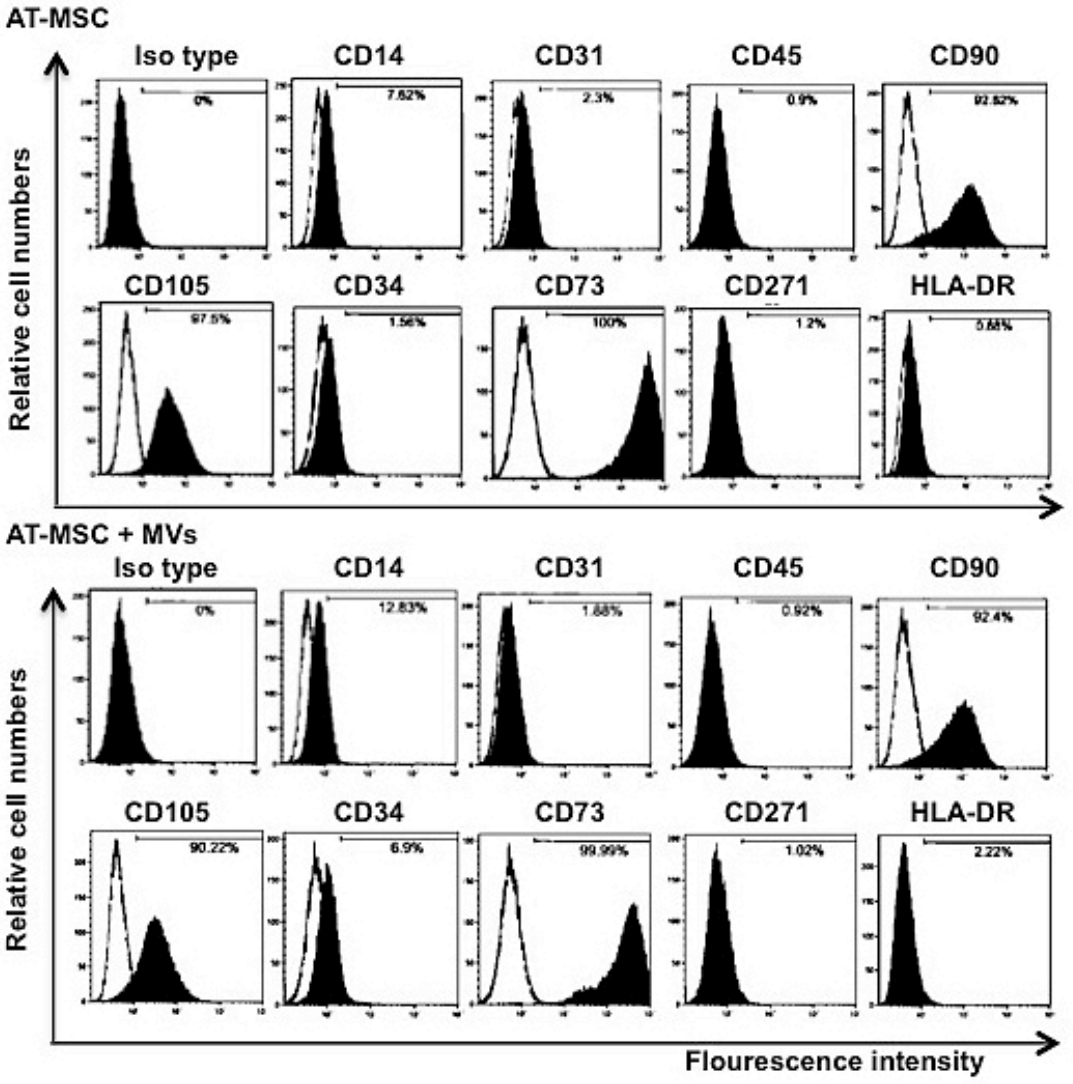

Figure 16. Comparison of cell surface markers between AT-MSCs and AT-MSCs transfected MVs derived from Alde-Low EPCs

FACS analysis of cell surface markers on AT-MSCs and AT-MSCs transfected MVs. Both were analyzed cell surface markers for CD14, CD31, CD45, CD90, CD105, CD34, CD73, CD271, HLA-DR.

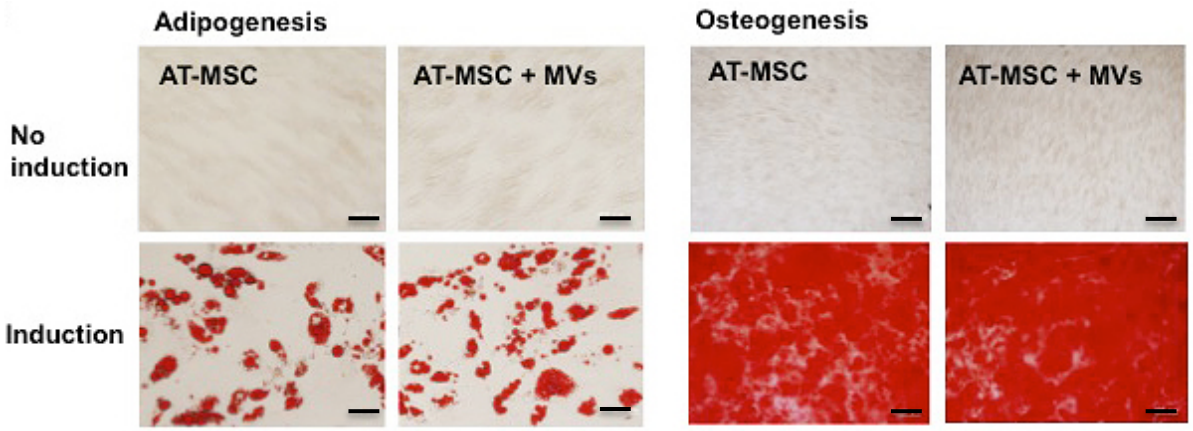

Figure 17. Comparison of differentiation capacity between AT-MSCs and AT-MSCs transfected MVs derived from Alde-Low EPCs

Each type of MSCs was analyzed to determine adipogenic and osteogenic differentiation potential. Adipogenesis was examined by the detection of lipid vacuoles by Oil Red O staining without induction (upper column) or with induction (below column), scale bar indicates 50μm. Osteogenesis was analyzed by Alizarin Red S staining without induction (upper column) or with induction (below column), scale bar indicates 200μm. There was no difference in AT-MSCs and AT-MSCs transfected MVs derived from Alde-Low EPCs.

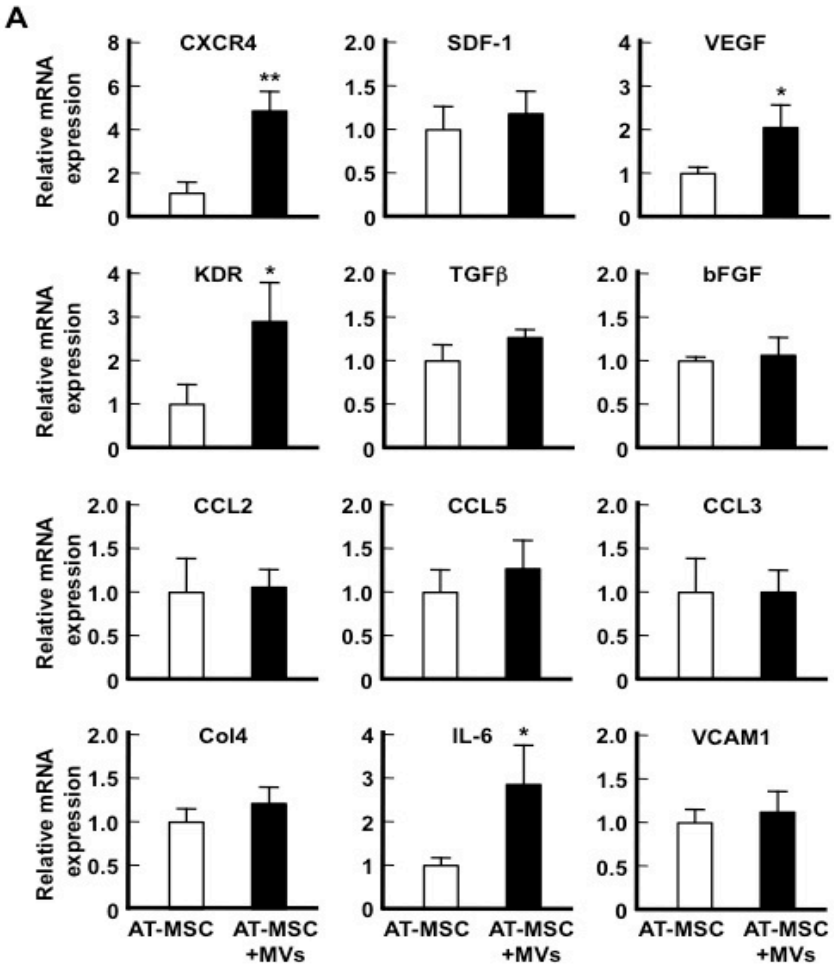

Figure 18. The expression of genes related to migration, angiogenesis, adhesion of AT-MSCs and AT-MSCs transfected MVs.

AT-MSCs were incubated with Alde-Low EPCs derived MVs for 12 h, then total mRNAs were extracted using Isogen following the procedure by the manufacturer. The gene expression profiles were analyzed by real-time polymerase chain reaction (ABI 7500Fast Real-time PCR system). *White bar* indicated AT-MSCs mock, *black bar* indicated AT-MSCs transfected with MVs. The expression levels AT-MSCs were normalized to a value of 1 as the standard for each factor. * $P<0.05$, ** $P<0.01$.

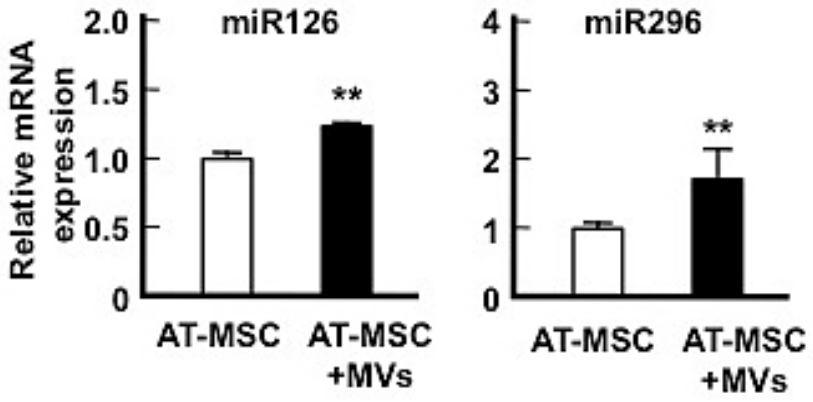

Figure 19. miRNA expression of AT-MSCs and AT-MSCs transfected MVs derived from Alde-Low EPCs

miR-126, miR-296 expression levels were upregulated in AT-MSCs transfected EPC-MVs in the normoxic condition. MVs derived from Alde-Low EPCs were incubated with AT-MSCs for 12 h. miRNAs were isolated and cDNAs were synthesized by using Taqman miRNA reverse transcription kit following the procedure suggested by the manufacturer. *White bar* indicate AT-MSCs, *black bar* indicate AT-MSCs treated EPC-MVs. The expression levels seen in AT-MSCs were normalized to a value of 1 as the standard for each factor. $^{**}P < 0.01$.

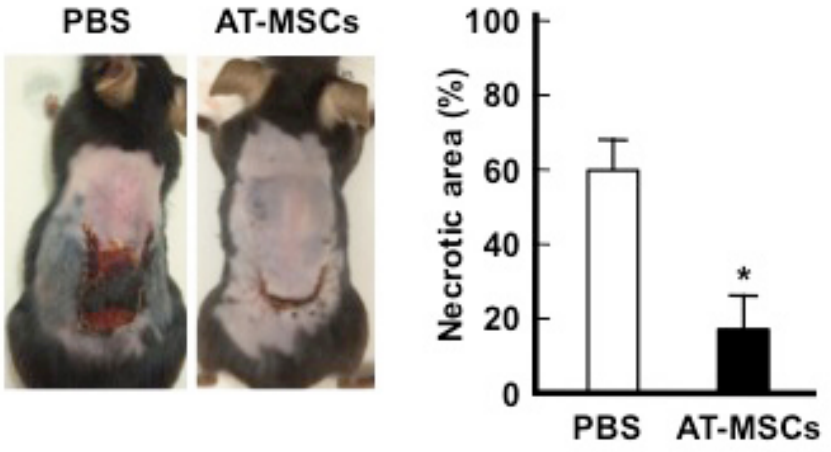

Figure 20. Mouse flap model by local injection of AT-MSCs

Skin incisions were created on the dorsal surfaces of mice, and control PBS and AT-MSCs were injected directly to skin. The effectiveness of PBS, AT-MSCs to recover tissue from ischemia was examined on day 7 following surgery. The necrotic regions in the 2 types of mice (n=3 in each) were measured. Note that the area of necrosis was smaller in the mice injected with AT-MSCs when comparing with mice injected PBS. The graph showed % of necrotic area, white bar indicated PBS injection, *white bar* indicates PBS, *black bar* indicates AT-MSCs injection. **P<0.05*.

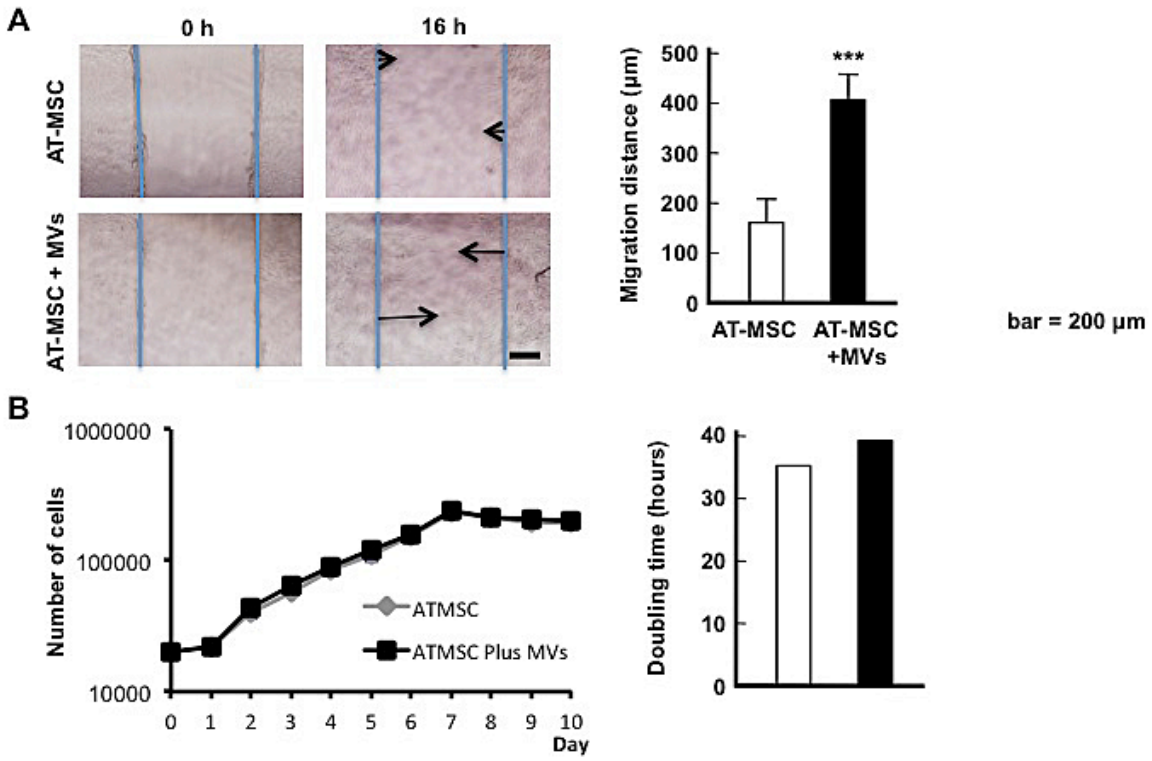

Figure 21. Alde-Low EPCs derived MVs enhanced the *in vitro* migration of AT-MSCs.

(**A)** AT-MSCs were plated to 100% confluent in 4-wells dish, then treated with 10µg/mL mytomicin C for 3 h in order to inhibit the proliferation of the cells. After washing 3 times by PBS, the wound 1mm in diameter was made by scraping with a 200µm Fisher-brand pipette tip. Cells were washed with PBS and imaged and subsequently incubated with MVs derived from Alde-Low EPCs. On the left side, the representative photograph of the wound edge at 0h and 16 h after incubating MVs

derived from Alde-Low EPCs (bar = 200μm). The migration distances were measure by software Image J. On the right side, migration distance (μm) of the AT-MSCs treated EPC-MVs significantly greater than the control AT-MSCs. *** $P < 0.001$.

(B) AT-MSCs treated with EPC-MVs and control AT-MSCs were plated at 20,000 cells/dish, then cell counting was performed everyday until day 10. The left side shows growth curve. The right side shows doubling time of the cells. No significant different of the proliferation were noticed (*white bar* indicates AT-MSCs, *black bar* indicates AT-MSCs transfected EPC-MVs).

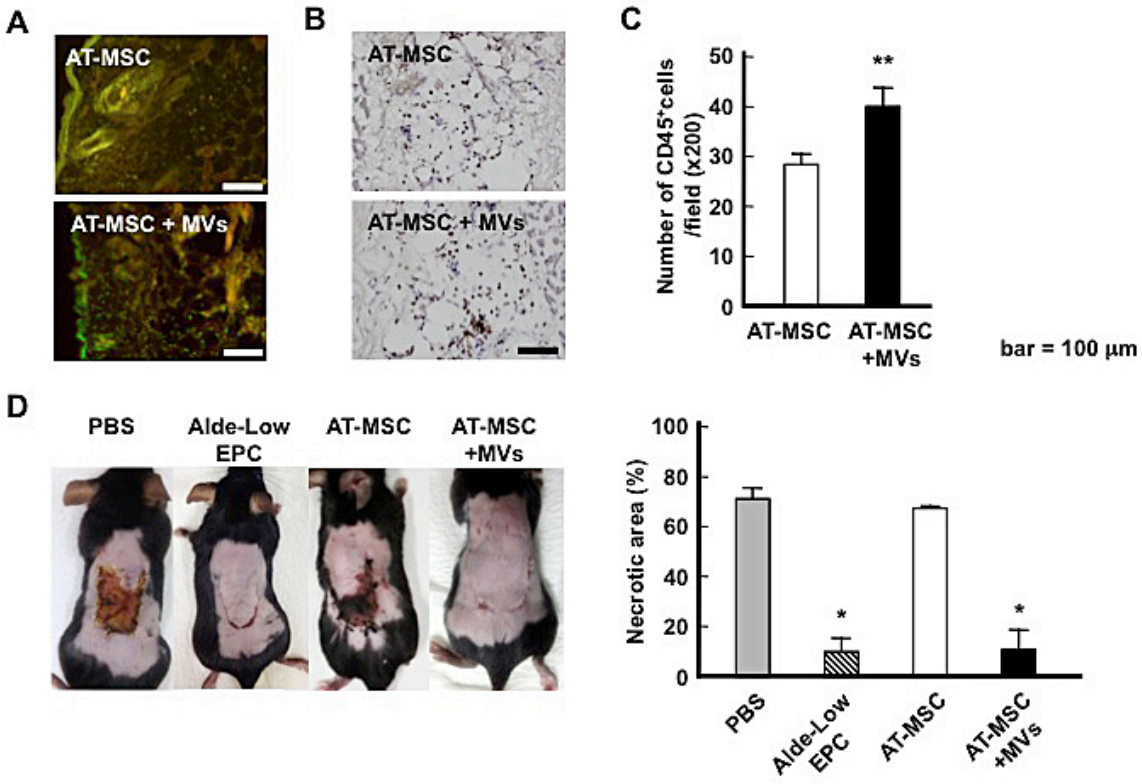

Figure 22. Alde-Low EPCs derived MVs enhanced the *in vivo* angiogenesis of AT-MSCs.

(**A)** Skin incisions were created on the dorsal surfaces of mice, then control AT-MSCs and ATMSCs treated with Alde-Low EPC-MVs were injected through tail vein (n=3). MVs derived from Alde-Low EPCs were stained by PKH67 (Green fluorescent) before the incubation with AT-MSCs. After 24 h injection of AT-MSCs or AT-MSCs treated EPC-MVs, lectin (red fluorescent) was injected through tail vein, then the back skin were collected and the frozen tissue sections were prepared. The fluorescent signals were detected under microscope. (Bar =100μm).

(**B, C)** After 3 days of cell-injection, the back skins of mice were prepared for making frozen sections. Immunohistochemistry was performed to detect CD45 positive cells. The graph shows the number of $CD45^+$ cells of AT-MSCs and AT-MSCs treated with EPC-MVs. **(D)** The effectiveness of PBS, Alde-Low EPCs, AT-MSCs and AT-MSCs treated with EPC-MVs on the tissue recovery from ischemia was examined on day 7 following surgery. The necrotic regions in each 4 types of mice (n=3) were measured. Note that the area of necrosis was significantly smaller in the mice injected with AT-MSCs transfected EPC-MVs when comparing with mice injected AT-MSCs. The graph shows % of necrotic area, grey bar indicates PBS injection, striped bar indicates Alde-Low EPCs injection, white bar indicates AT-MSCs injection and black bar indicates AT-MSCs transfected MVs. *$*P<0.05$, **$**P<0.01$.

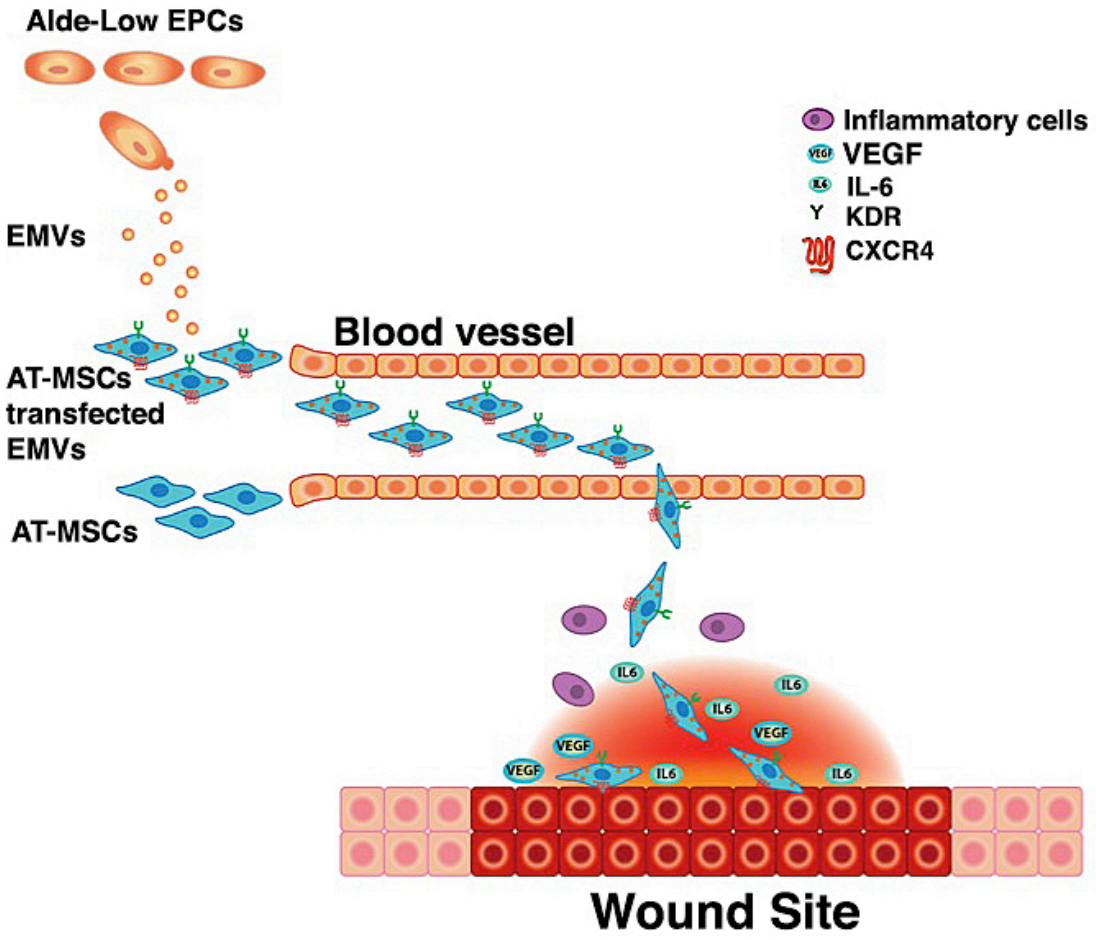

Fig. 23. Scheme of the Alde-Low EPCs derived MVs function to support wound healing of AT-MSCs

A schematic drawing review the hypothesis of the function of MVs derived from Alde-Low EPCs to enhance migratory ability of AT-MSCs, resulting in wound healing.

Acknowledgments

Firstly, I would like to express my sincere gratitude to my advisor Prof. Osamu Ohneda for the greatest support of my Ph.D study and related research, for his patience, motivation, and immense knowledge. His guidance helped me in all the time of research and writing of this thesis.

Besides my advisor, I would like to thank you Assistant Prof. Dr. Takasaki, Assistant Prof. Yamashita and Dr. Nagano for their insightful comments and encouragement, but also for the hard question which incented me to widen my research from various perspectives.

I would like to thank you thesis committee members Sugiyama Sensei, Suzuki Sensei, Segawa Sensei, Hamada Sensei for their valuable comments and evaluation and also for the hard questions which help me to perfect my doctoral dissertation as well as to improve knowledge.

I thank my dear lab members in for the stimulating discussions, for the sleepless nights we were working together before deadlines, and for all the fun we have had in the last five years. I want to thank Satomi, Tsuboi, Akimoto, Kimura, Kato, Khanh for their help. During PhD course, I want to thank my little sister Thuy for her sharing while we work and live together.

I would like to thank you all members and staffs of Medical area offices, International offices for providing information as well as kind supports during my stay in Tsukuba.

I would like to thank you Japanese Government MEXT Scholarship as well as Otsuka Toshimi Scholarship Foundation for the finance support.

In addition, I would like to thank Director of home Institute – Institute of Tropical Biology- Dr. Son for his support during my Ph.D study.

Besides, I thank all my friends in Japan, especially Vietnamese friends for sharing and enjoying every moments of life in day or night, in happiness or sadness. Our memories will stay forever.

Certainly, I thank my old students, friends in Viet Nam for their help and support during five years.

Last but not the least, I would like to special thank my family: my greatest mother for bringing me to this world, thank you for her love and encouragement. Moreover, I thank you two beloved daughters as well as my hubby for supporting me spiritually throughout doing researches, writing paper as well as thesis and my life in general.

Tsukuba, July 12th, 2016

TRAN CAM TU

参　考　論　文

References

[1]. T. Asahara, T. Murohara, A. Sullivan. (1997). Isolation of putative progenitor endothelial cells for angiogenesis. Science; 275: 964–7.

[2]. Q. Shi, S. Rafii, M.H. Wu. (1998). Evidence for circulating bone marrow-derived endothelial cells. Blood; 92: 362–367.

[3]. T. Asahara, H. Masuda, T. Takahashi. (1999). Bone marrow origin of endothelial progenitor cells responsible for postnatal vasculogenesis in physiological and pathological neovascularization. Circ Res; 85: 221–228.

[4]. J. Folkman, Y. Shing. (1992). Angiogenesis. J Biol Chem; 267: 10931–10934.

[5]. D.A. Ingram, N.M. Caplice, M.C. Yoder. (2005). Unresolved questions, changing definitions, and novel paradigms for defining endothelial progenitor cells. Blood; 106: 1524-1531.

[6]. J. Hur, C.H. Yoon, H.S. Kim. (2004). Characterization of two types of endothelial progenitor cells and their different contributions to neovasculogenesis. Arterioscler Thromb Vasc Biol; 24: 288-293.

[7]. M.C. Yoder, L.E. Mead, D. Prater. (2007). Re-defining endothelial progenitor cells via clonal analysis and hematopoietic stem/progenitor cell principals. Blood; 109: 1801-1809.

[8]. D.A. Ingram, L.E. Mead, H. Tanaka. (2004). Identification of a novel hierarchy of endothelial progenitor cells using human peripheral and umbilical cord blood. Blood; 104: 2752-2760.

[9]. B. Jackson, C. Brocker, D.C. Thompson, W. Black, K. Vasiliou, D.W. Nebert, V. Vasiliou. (2011). Update on the aldehyde dehydrogenase gene (ALDH) superfamily. Hum Genomics; 5: 283–303.

[10]. N.A. Sophos, V. Vasiliou. (2003). Aldehyde dehydrogenase gene superfamily: the 2002 update. Chem Biol Interact; 22: 143–144.

[11]. R.W. Storms, A.P. Trujillo, J.B. Springer. (1999). Isolation of primitive human hematopoietic progenitors on the basis of aldehyde dehydrogenase activity. Proc Natl Acad Sci U S A; 96: 9118-9123.

[12]. J.E. Russo, J. Hilton. (1988). Characterization of cytosolic aldehyde dehydrogenase from cyclophosphamide resistant L1210 cells. Cancer Res; 48: 2963-2968.

[13]. J. Labrecque, P.V. Bhat, A. Lacroix. (1993). Purification and partial characterization of a rat kidney aldehyde dehydrogenase that oxidizes retinal to retinoic acid. Biochem Cell Biol; 71: 85-89.

[14]. T.G. Flynn, J.E. Weiner, H. Russo, J. Hilton, O.M. Colvin. (1989). The role of aldehyde dehydrogenase isozymes in cellular resistance to the alkylating agent cyclophosphamide. Enzymology and Molecular Biology of Carbonyl Metabolism; 2: 65-79.

[15]. R.J. Jones, J.P. Barber, M.S. Val. (1995). Assessment of aldehyde dehydrogenase in viable cells. Blood; 85: 2742-2746.

[16]. T.G. Flynn, H. Weiner, J.E. Russo, J. Hilton, O.M. Colvin. (1989). The role of aldehyde dehydrogenase isozymes in cellular resistance to the alkylating agent cyclophosphamide. In: T.G. Flynn, H. Weiner, editors. Enzymology and Molecular Biology of Carbonyl Metabolism 2. New York, NY: Alan R. Liss: 65-79.

[17]. L. Armstrong, M. Stojkovic, I. Dimmick. (2004). Phenotypic characterization of murine primitive hematopoietic progenitor cells isolation on the basis of aldehyde dehydrogenase activity. Stem Cells; 22: 1142-1151.

[18]. M. Nagano, T. Yamashita, H. Hamada, K. Ohneda, K. Kimura, T. Nakagawa, M. Shibuya, H. Yoshikawa, O. Ohneda. (2007). Identification of functional endothelial progenitor cells suitable for the treatment of ischemic tissue using human umbilical cord blood. Blood; 110: 151–160.

[19]. A. Aicher, A. M. Zeiher, S. Dimmeler. (2005). Mobilizing endothelial progenitor Cells. Hypertension; 45: 321-325.

[20]. D. Shweiki, A. Itin, D. Soffer, E. Keshet. (1992). Vascular endothelial growth factor induced by hypoxia may mediate hypoxia-initiated angiogenesis. Nature; 359: 843-845.

[21]. T. Asahara, T. Takahashi, H. Masuda, C. Kalka, D. Chen, H. Iwaguro, Y. Inai, M. Silver, J. M. Isner. (1999). VEGF contributes to postnatal

neovascularization by mobilizing bone marrow-derived endothelial progenitor cells. EMBO Molecular Medicine; 18: 3964-3972.

[22]. C. Heeschen, A. Aicher, R. Lehmann, S. Fichtlscherer, M. Vasa, C. Urbich, C. Mildner-Rihm, H. Martin, A. M. Zeiher, S. Dimmeler. (2003). Erythropoietin is a potent physiologic stimulus for endothelial progenitor cell mobilization. Blood; 102: 1340-1346.

[23]. F. H. Bahlmann, K. Groot, JM. Spandau, A. L. Landry, B. Hertel, T. Duckert, S. M. Boehm, J. Menne, H. Haller, D. Fliser. (2004). Erythropoietin regulates endothelial progenitor cells. Blood; 103: 921-926.

[24]. O.M. Tepper, J.M. Capla, R.D. Galiano, D.J. Ceradini, M.J. Callaghan, M.E. Kleinman, G.C. Gurtner. (2005). Adult vasculogenesis occurs through in situ recruitment, proliferation, and tubulization of circulating bone marrow-derived cells. Blood; 105:1068–1077.

[25]. Mihail Hristov, Wolfgang Erl, Peter C. Weber. (2003). Endothelial Progenitor Cells. Mobilization, Differentiation, and Homing Arterioscler Thromb Vasc Biol; 23: 1185-1189.

[26]. P. Vajkoczy, S. Blum, M. Lamparter, R. Mailhammer, R. Erber, B. Engelhardt, D. Vestweber, K. Hatzopoulos. (2003). Multistep nature of microvascular recruitment of ex vivo expanded embryonic endothelial progenitor cells during tumor angiogenesis. The Journal of Experimental Medicine; 197: 1755-1765.

[27]. E. Chavakis, A. Aicher, C. Heeschen, K. Sasaki, R. Kaiser, Naual E. Makhfi, C. Urbich, T. Peters, K. S. Kochanek, A. M. Zeiher, T. Chavakis, S. Dimmeler. (2005). Role of Beta 2-integrins for homing and neovascularization capacity of endothelial progenitor cells. The Journal of Experimental Medicine; 201: 63-72.

[28]. C. Kalka, H. Masuda, T. Takahashi, R. Gordon, O. Tepper, E. Gravereaux, A. Pieczek, H. Iwaguro, S. Hayashi, J. M. Isner, T. Asahara. (2000). Vascular Endothelial Growth Factor165 gene transfer augments circulating endothelial progenitor cells in human subjects. Circulation Research; 86: 1198-1202.

[29]. J. Yamaguchi, KF. Kusano, O. Masuo, A. Kawamoto, M. Silver, S. Murasawa, M. Bosch-Marce, H. Masuda, DW. Losordo, JM. Isner, T. Asahara. (2003). Stromal Cell Derived Factor-1 effects on ex vivo expanded endothelial progenitor cell recruitment for ischemic neovascularization. Circulation; 107: 1322-1328.

[30]. M. Kucia, K. Jankowski, R. Reca, M. Wysoczynski, L. Bandura, D. J. Allendorf, J. Zhang, J. Ratajczak, M. Z. Ratajczak. (2004). CXCR4–SDF-1 Signalling, Locomotion, Chemotaxis and Adhesion. J Molecular Histology; 35: 233-245.

[31]. F. Timmermans, J. Plum, M.C. Yoder, D.A. Ingram, B. Vandekerckhove, J. Case. (2009). Endothelial progenitor cells: identity defined? J Cell Mol Med; 13: 87–102.

[32]. M. Jiang, B. Wang, C. Wang, B. He, H. Fan, T.B. Guo, Q. Shao, L. Gao, Y. Liu. (2008). Angiogenesis by transplantation of HIF-1 alpha modified EPCs into ischemic limbs. J Cell Biochem; 103: 321–334.

[33]. T. Asahara, A. Kawamoto. (2004). Endothelial progenitor cells for postnatal vasculogenesis. Am J Physiol Cell Physiol; 287: 572–579.

[34]. D.J. Ceradini, A.R. Kulkarni, M.J. Callaghan, O.M. Tepper, N. Bastidas, M.E. Kleinman, J.M. Capla, R.D. Galiano, J.P. Levine, G.C. Gurtner. (2004). Progenitor cell trafficking is regulated by hypoxic gradients through HIF-1 induction of SDF-1. Nat Med; 10: 858–864.

[35]. M. Pesce, A. Orlandi, M.G. Iachininoto, S. Straino, A.R. Torella, V. Rizzuti, G. Pompilio, G. Bonanno, G. Scambia, M.C. Capogrossi. (2003). Myoendothelial differentiation of human umbilical cord blood-derived stem cells in ischemic limb tissues. Circ Res; 93: e51–e62.

[36]. C. Alev, M. Ii, T. Asahara. (2011). Endothelial progenitor cells: a novel tool for the therapy of ischemic diseases. Antioxid Redox Signal; 15: 949–965.

[37]. J. Ratajczak, M. Wysoczynski, F. Hayek, A. Janowska-Wieczorek, M.Z. Ratajczak. (2006). Membrane-derived microvesicles: important and underappreciated mediators of cell-to-cell communication. Leukemia; 20: 1487–1495.

[38]. M.C. Deregibus, V. Cantaluppi, R. Calogero, M.L. Iacono, C. Tetta, L. Biancone, S. Bruno, B. Bussolati, G. Camussi. (2007). Endothelial

progenitor cell derived microvesicles activate an angiogenic program in endothelial cells by a horizontal transfer of mRNA. Blood; 110: 2440–2448.

[39]. S. Gu, W. Zhang, J. Chen, R. Ma, X. Xiao, X. Ma, Z. Yao, Y. Chen. (2014). EPC-derived microvesicles protect cardiomyocytes from Ang II-induced hypertrophy and apoptosis. PLoS One 9: e85396.

[40]. C. W. Pugh, P. J. Ratcliffe. (2003). Regulation of angiogenesis by hypoxia: role of the HIF system. Nature Medicine; 9: 677 - 684

[41]. K. S. Hewitson , C. J. Schofield. (2004). The HIF pathway as a therapeutic target. Drug Discove Today; 9: 704-711.

[42]. D.J. Prockop. (1997). Marrow stromal cells as stem cells for nonhematopoietic tissues. Science; 276: 71–74.

[43]. D.C. Colter, R. Class, C.M. DiGirolamo. (2000). Rapid expansion of recycling stem cells in cultures of plastic-adherent cells from human bone marrow. Proc Natl Acad Sci USA; 97: 3213–3218.

[44]. C. Campagnoli, I.A. Roberts, S. Kumar. (2001). Identification of mesenchymal stem/progenitor cells in human first-trimester fetal blood, liver, and bone marrow. Blood; 98: 2396–2402.

[45]. P.S. In't Anker, S.A. Scherjon, C. Kleijburg-van der Keur. (2003). Amniotic fluid as a novel source of mesenchymal stem cells for therapeutic transplantation. Blood; 102: 1548–1549.

[46]. P.A Zuk, M. Zhu, P. Ashjian. (2002). Human adipose tissue is a source of multipotent stem cells. Mol Biol Cell; 13: 4279–4295.

[47]. T.C. Tu, K. Kenichi, N. Masumi, Y. Toshiharu, O. Kinuko, S. Haruhiko, S. Fujio, S. Yuzuru, H. Hiromi, Y. Hiroyuki, H.N. Son, O. Ohneda. (2010). Identification of human placenta-derived mesenchymal stem cells involved in re-endothelialization. J. Cell. Physiol; 226: 224–235.

[48]. M. Körbling, Z. Estrov. (2003). Adult stem cells for tissue repair - a new therapeutic concept? N. Engl. J. Med; 349: 570-582.

[49]. M. Körbling, Z. Estrov, R. Champlin, (2003). Adult stem cells and tissue repair. Bone Marrow Transplant; 32: 23–24.

[50]. P.L. Weissberg, A. Qasim, (2005). Stem cell therapy for myocardial repair. Heart; 91: 696-702.

[51]. A. Kawamoto, D. W. Losordo (2008). Endothelial Progenitor Cells for Cardiovascular Regeneration, Trends Cardiovasc. Med.; 18: 33-37.

[52]. T. Asahara, T. Murohara, A. Sullivan, M. Silver, R. van der Zee, T. Li, B. Witzenbichler, G. Schatteman, J.M. Isner. (1997). Isolation of Putative Progenitor Endothelial Cells for Angiogenesis. Science; 275: 964-967.

[53]. Susan M. van Dommelen, Pieter Vader, Samira Lakhal, S.A.A. Kooijmans, Wouter W. van Solinge, Matthew J.A. Wood, Raymond M. Schiffelers. (2012). Microvesicles and exosomes: Opportunities for cell-derived

membrane vesicles in drug delivery. Journal of Controlled Release; 161: 635-644

[54]. T.C. Tu, M. Nagano, T. Yamashita, H. Hamada, K. Ohneda, K. Kimura, O. Ohneda. (2016). A chemokine receptor, CXCR4, which is regulated by hypoxia-inducible factor 2a, is crucial for functional endothelial progenitor cells migration to ischemic tissue and wound repair. Stem Cells Dev; 25: 266-276.

[55]. M. Morita, O. Ohneda, T. Yamashita, S. Takahashi, N. Suzuki, O. Nakajima, S. Kawauchi, M. Ema, S. Shibahara. (2003). HLF/HIF-2alpha is a key factor in retinopathy of prematurity in association with erythropoietin. EMBO J; 22: 1134–1146.

[56]. S. Boyden. (1962). The chemotactic effect of mixtures of antibody and antigen on polymorphonuclear leucocytes. J. Exp. Med; 115: 453–466.

[57]. I. Kratchmarova, B. Blagoev, M. Haack-Sorensen, M. Kassem, M. Mann, (2005). Mechanism of divergent growth factor effects in mesenchymal stem cell differentiation. Science; 308: 1472-1477.

[58]. K. Kimura, M. Nagano, G. Salazar, T. Yamashita, I. Tsuboi, H. Mishima, S. Matsushita, F. Sato, K. Yamagata, O. Ohneda. (2014). The role of CCL5 in the ability of adipose tissue-derived mesenchymal stem cells to support repair of ischemic regions. Stem Cells Dev; 23: 488–501.

[59]. C.C. Liang, A.Y. Park, J.L. Guan. (2007). In vitro scratch assay: a convenient and inexpensive method for analysis of cell migration in vitro. Nature Protocols; 2: 329-333.

[60]. S. Bruno, C. Grange, M.C. Deregibus, R.A. Calogero, S. Saviozzi, F. Collino, L. Morando, A. Busca, M. Falda. (2009). Mesenchymal stem cell-derived microvesicles protect against acute tubular injury. J Am Soc Nephrol; 20: 1053–1067.

[61]. L. Li, D. Zhu, L. Huang, J. Zhang, Z. Bian, X. Chen, Y. Liu, C.Y. Zhang, K. Zen. (2012). Argonaute 2 complexes selectively protect the circulating microRNAs in cell-secreted microvesicles. PLoS One; 7: e46957.

[62]. D.A. Ingram, L.E. Mead, H. Tanaka, V. Meade, A. Fenoglio, K. Mortell, K. Pollok, M.J. Ferkowicz, D. Gilley, M.C. Yoder. (2004). Identification of a novel hierarchy of endothelial progenitor cells using human peripheral and umbilical cord blood. Blood; 104: 2752–2760.

[63]. A. Ranghino, V. Cantaluppi, C. Grange, L. Vitillo, F. Fop, L. Biancone, M.C. Deregibus, C. Tetta, G.P. Segoloni, G. Camussi. (2012). Endothelial progenitor cell-derived microvesicles improve neovascularization in a murine model of hindlimb ischemia. Int J Immunopathol Pharmacol; 25: 75–85.

[64]. V. Cantaluppi, S. Gatti, D. Medica, F. Figliolini, S. Bruno, M.C. Deregibus, A. Sordi, L. Biancone, C. Tetta, G. Camussi. (2012). Microvesicles derived

from endothelial progenitor cells protect the kidney from ischemia–reperfusion injury by microRNA-dependent reprogramming of resident renal cells. Kidney Int; 82: 412–427.

[65]. T. Würdinger, B.A. Tannous, O. Saydam, J. Skog, S. Grau, J. Soutschek, R. Weissleder, X.O. Breakefield, A.M. Krichevsky. (2008). miR-296 regulates growth factor receptor overexpression in angiogenic endothelial cells. Cancer Cell; 14: 382–393.

[66]. S. Wang, A.B. Aurora, B.A. Johnson, X. Qi, J. McAnally, J.A. Hill, J.A. Richardson, R. Bassel-Duby, E.N. Olson. (2008). The endothelial-specific microRNA miR-126 governs vascular integrity and angiogenesis. Dev Cell; 15: 261–271.

[67]. M.R. Hoenig, C. Bianchi, A. Rosenzweig, F.W. Sellke. (2008). Decreased vascular repair and neovascularization with ageing: mechanisms and clinical relevance with an emphasis on hypoxia-inducible factor-1. Curr Mol Med; 8: 754–767.

[68]. J.M. Isner, C. Kalka, A. Kawamoto, T. Asahara. (2001). Bone marrow as a source of endothelial cells for natural and iatrogenic vascular repair, Ann. N.Y. Acad. Sci.; 953: 75-84.

[69]. T. Takahashi, C. Kalka, H. Masuda, D .Chen, M. Silver, M. Kearney, M. Magner, J.M. Isner, T. Asahara. (1999). Ischemia- and cytokine-induced

mobilization of bone marrow-derived endothelial progenitor cells for neovascularization. Nat. Med.; 5: 434-438.

[70]. O. Ohneda, M. Nagano, Y. Fuji-Kuriyama. (2007). Role of hypoxia-inducible factor-2alpha in endothelial development and hematopoiesis. Methods Enzymol; 435: 199–218.

[71]. H.E. Ryan, J. Lo, R.S. Johnson. (1998). HIF-1 alpha is required for solid tumor formation and embryonic vascularization. EMBO J; 17: 3005–3015.

[72]. S. Bruno, C. Grange, F. Collino, M.C. Deregibus, V. Cantaluppi, L. Biancone, C. Tetta, G. Camuss. (2012). Microvesicles derived from mesenchymal stem cells enhance survival in a lethal model of acute kidney injury. PLoS ONE 7: e33115.

[73]. F.P. Barry, J.M. Murphy. (2004). Mesenchymal stem cells: clinical applications and biological characterization. Int. J. Biochem. Cell Biol; 36: 568–584.

[74]. I. Kratchmarova, B. Blagoev, M. Haack-Sorensen, M. Kassem, M. Mann. (2005). Mechanism of divergent growth factor effects in mesenchymal stem cell differentiation. Science; 308: 1472-1477.

[75]. D.P. Bartel. (2004). MicroRNAs: genomics, biogenesis, mechanism, and function. Cell; 116: 281–297.

[76]. JJ. Chen, SH. Zhou. (2011). Mesenchymal stem cells overexpressing miR-126 enhance ischemic angiogenesis via the AKT/ERK-related pathway. Cardiol J; 18: 675–681.

[77]. T. Würdinger, B. A. Tannous, O. Saydam, J. Skog, St. Grau, J. Soutschek, R. Weissleder, X. O. Breakefield, A. M. Krichevsky. (2008). miR-296 Regulates Growth Factor Receptor Overexpression in Angiogenic Endothelial Cells. Cancer cell; 14: 382-393.

[78]. Y. Wu, L. Chen, P.G. Scott, E.E. Tredget. (2007). Mesenchymal stem cells enhance wound healing through differentiation and angiogenesis. Stem Cells; 25: 2648-2659.

[79]. S. Bruno, C. Grange, F. Collino, M.C. Deregibus, V. Cantaluppi, L. Biancone, C. Tetta, G. Camuss. (2012). Microvesicles derived from mesenchymal stem cells enhance survival in a lethal model of acute kidney injury. PLoS ONE; 7: e33115.

[80]. S. Bruno, F. Collino, M.C. Deregibus, C. Grange, C. Tetta, G. Camussi. (2013). Microvesicles derived from human bone marrow mesenchymal stem cells inhibit tumor growth. Stem Cells Dev; 22: 758-771.

[81]. L. Chen, E.E. Tredget, P.Y. Wu, Y. Wu. (2008). Paracrine factors of mesenchymal stem cells recruit macrophages and endothelial lineage cells and enhance wound healing. PLoS ONE; 3: e1886.

[82]. Y. Gheisari, K. Azadmanesh, N. Ahmadbeigi, S.M. Nassiri, A.F. Golestaneh, M. Naderi, M. Vasei, E. Arefian, S. Mirab-Samiee, A. Shafiee, M. Soleimani, S. Zeinali. (2012). Genetic modification of mesenchymal stem cells to overexpress CXCR4 and CXCR7 does not improve the homing and therapeutic potentials of these cells in experimental acute kidney injury. Stem Cells and Dev; 21: 2969-2980.

[83]. F. Tögel, A. Cohen, P. Zhang, Y. Yang, Z. Hu, C. Westenfelder. (2009). Autologous and allogeneic marrow stromal cells are safe and effective for the treatment of acute kidney injury. Stem Cells and Dev; 18: 475-486.

[84]. K. L. Pricola, N. Z. Kuhn, H. Haleem-Smith, R. S. Tuan. (2009). Interleukin-6 maintains bone marrow-derived mesenchymal stem cell stemness by an ERK1/2-dependent mechanism. J. Cell. Biochem; 108: 577–588.

[85]. R. Jaiswal, F. Luk, J. Gong, J.M. Mathys, G.E. Grau, M. Bebawy. (2012). Microparticle conferred micro- RNA profiles–implications in the transfer and dominance of cancer traits. Mol Cancer; 11: 37.

[86]. M. Yang, J. Chen, F. Su, B. Yu, F. Su, L. Lin. (2011). Microvesicles secreted by macrophages shuttle invasion-potentiating microRNAs into breast cancer cells. Mol Cancer; 10:117.

[87]. M. Hulsmans, P. Holvoet. (2013). MicroRNA-containingmicrovesicles regulating inflammation in association with atherosclerotic disease. Cardiovascular Research; 100: 7–18.

[88]. S. Djuranovic, A. Nahvi, R. Green. (2011). Aparsimonious model for gene regulation by miRNAs. Science; 331: 550–553.

[89]. D.P. Bartel. (2004). MicroRNAs: genomics, biogenesis, mechanism, and function. Cell; 116: 281–297.

[90]. V. Cantaluppi, S. Gatti, D. Medica, F. Figliolini, S. Bruno, M.C. Deregibus, A. Sordi, L. Biancone, C. Tetta, G. Camussi. (2012). Microvesicles derived from endothelial progenitor cells protect the kidney from ischemia–reperfusion injury by microRNA-dependent reprogramming of resident renal cells. Kidney Int; 82: 412–427.

Published publications

1. **Tran Cam Tu**, Masumi Nagano, Toshiharu Yamashita, Hiromi Hamada, Kinuko Ohneda, Kenichi Kimura, Osamu Ohneda, A chemokine receptor, CXCR4, which is regulated by hypoxia-inducible factor 2α, is crucial for functional endothelial progenitor cells migration to ischemic tissue and wound repair. Stem Cells Dev., 25 (2016) 266-276.
2. **Tran Cam Tu,** Toshiharu Yamashita, Toshiki Kato, Masumi Nagano, Nhu Thuy Trinh, Hiromi Hamada, Fujio Sato, Kinuko Ohneda, Mami Matsuo-Takasaki, Osamu Ohneda. Microvesicles derived from Alde-Low EPCs support the wound healing capacity of AT-MSCs. Biochemical and Biophysical Research Communications, 477 (2016) 68-75.